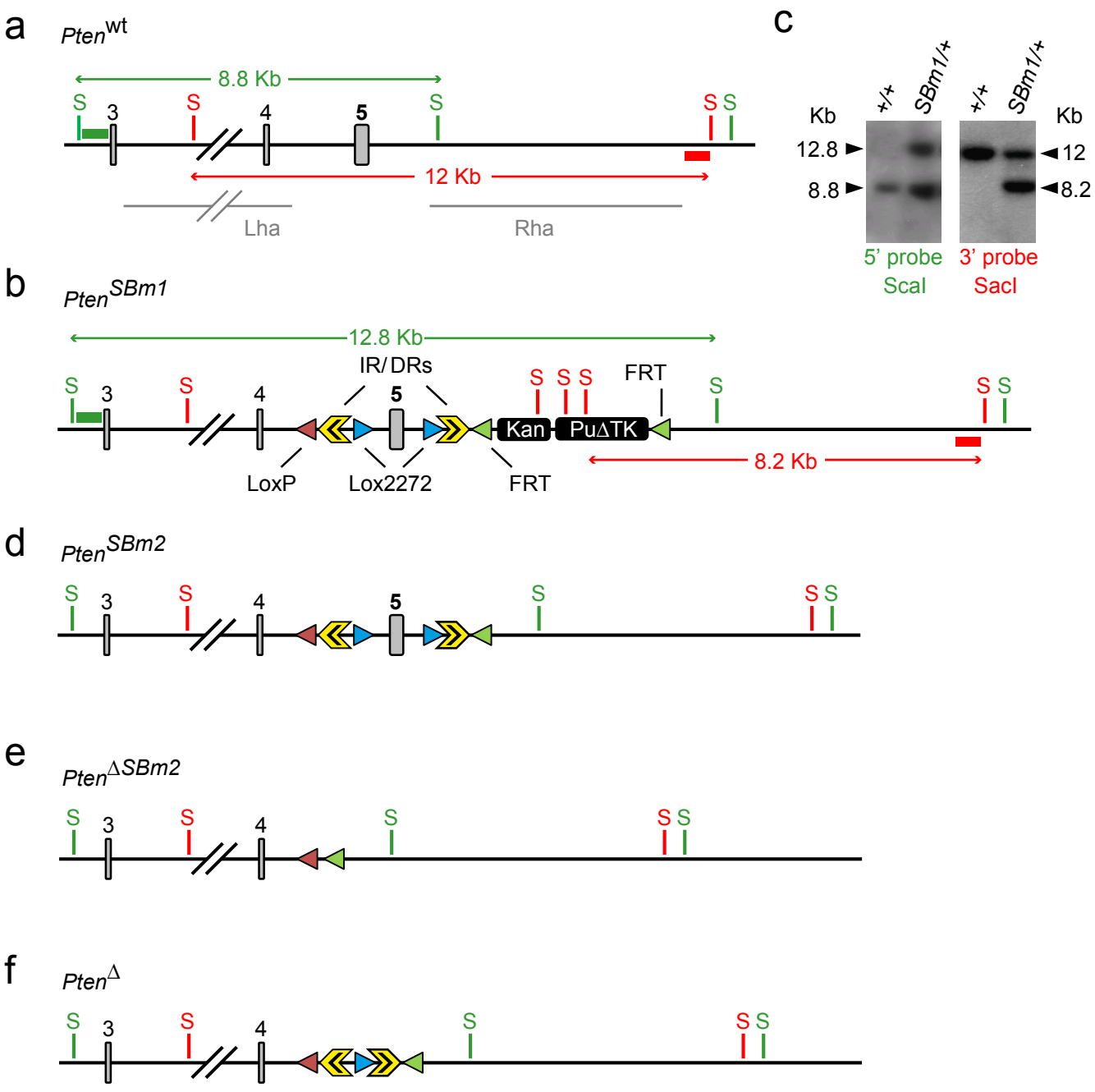

Supplementary Figure 1

Supplementary Figure 1. Schematic representation of the generation of the *Sleeping Beauty*-dependent inactivatable *Pten* allele. **(a)** Wild-type mouse *Pten* locus ($Pten^{wt}$). Grey boxes: exons; Lha/Rha: left and right homology arms; green rectangle: 5' probe; red rectangle: 3' probe. **(b)** Targeted *Pten* allele before removal of resistance cassette ($Pten^{SBm1}$). *Pten* exon 5 was flanked by two 5'-inverted terminal repeats of SB. Restriction sites relevant for the Southern-blot based screening are represented. Kan: kanamycin resistance cassette; PuΔTK: puromycin resistance cassette. **(c)** Southern-blot analysis of successfully targeted $Pten^{SBm1}$ clones. 5' (left) and 3' (right) screenings are shown. **(d)** Targeted *Pten* allele after removal of resistance cassette ($Pten^{SBm2}$). When F1 males heterozygous for the $Pten^{SBm1}$ allele are mated with $Rosa26^{FlpE/FlpE}$ to remove the FRT-flanked PuΔTK, offspring with the $Pten^{SBm2}$ conditional allele is generated. **(e)** Targeted *Pten* allele after transposon mobilization ($Pten^{\Delta SBm2}$). Mice with the $Pten^{SBm2}$ allele can be crossed to mice carrying the SB transposase to allow mobilization of the *Pten* exon 5 transposon, thus generating a *Pten* null allele ($Pten^{\Delta SBm2}$) and an additional mutation elsewhere in the genome if reintegration of the transposon occurs. **(f)** Targeted *Pten* allele after Cre mediated recombination ($Pten^{\Delta}$). The $Pten^{SBm2}$ allele can be used as Cre-conditional *Pten* allele, based on the presence of two Lox2272 sites flanking the essential *Pten* exon 5.

a

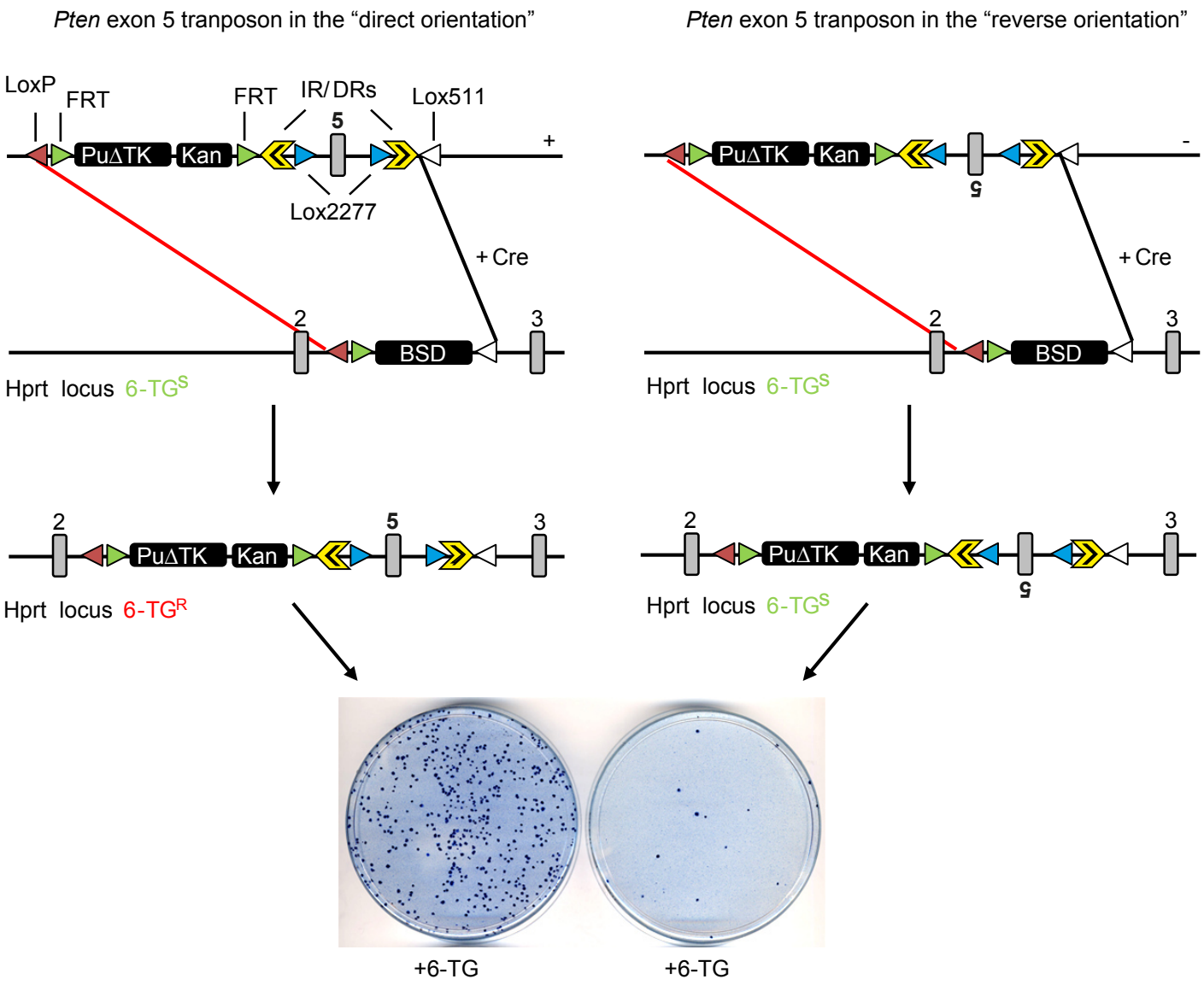

b

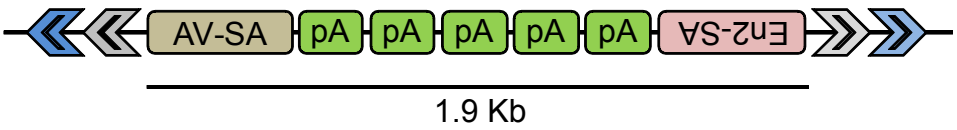

Supplementary Figure 2

Supplementary Figure 2. Inactivating capacity of the *Pten* exon 5 transposon and genetic structure of the ITP2m transposable element. **(a)** To ascertain the inactivating ability of the SB transposon harboring *Pten* exon 5 and surrounding intronic sequences as its only cargo, we performed an *Hprt* trapping assay. Two constructs with the *Pten* exon 5 transposon in the direct (left side of the figure) or reverse (right side of the figure) orientations were targeted into the X-linked *Hprt* locus in male ES cells. Then, cells were grown in the presence of 6-Thioguanine (6-TG), allowing for selection of *Hprt*-deficient cells. 6-TG resistant colonies are shown at the bottom of the figure. The transposon showed inactivating ability in the direct orientation (left plate) but nearly no trapping activity in the reverse orientation (right plate). **(b)** Structure of the ITP2m transposon. The ITP2m transposon is composed of one Adenovirus (AV-SA) and one Engrailed 2 (En2-SA) splice acceptors flanking five bi-directional polyadenylation signals. This cassette is flanked by *PiggyBac* (blue arrows) and *Sleeping Beauty* (grey arrows) terminal repeats, allowing transposon mobilization by both transposases. In total, the cargo size of the transposon is 1.9 Kb. ITP2m mouse lines carry around 35 copies of this inactivating transposon in chromosome 14.

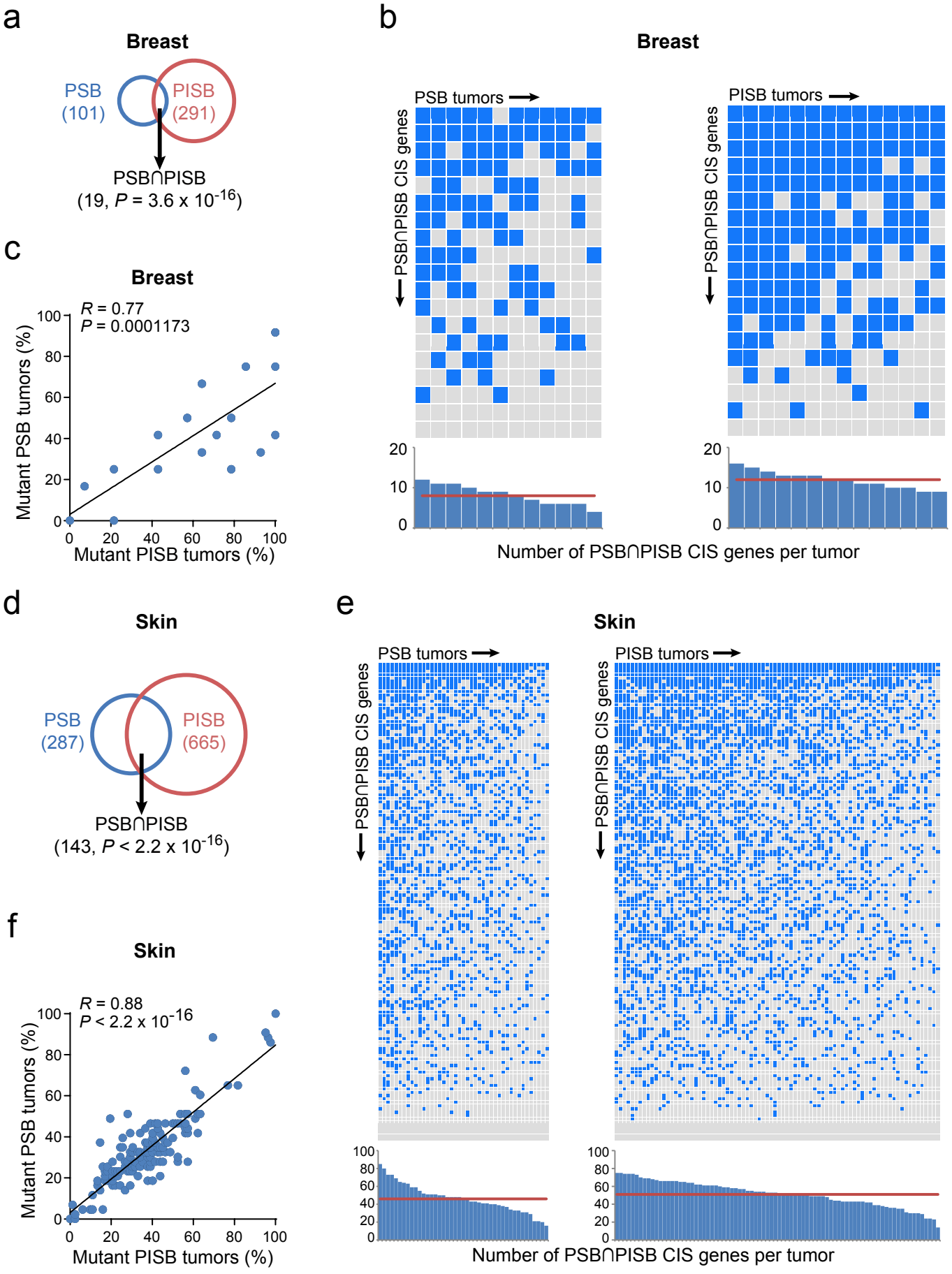

Supplementary Figure 3

Supplementary Figure 3. Analysis of PSB∩PISB CIS genes identified in breast and skin tumors. **(a)** Overlap between PSB (n=101) and PISB (n=291) CIS genes identified in breast tumors. *P* value was calculated using a two-by-two contingency table and Fisher's exact test. **(b)** Distribution of overlapping breast CIS genes (n=19) between PSB and PISB screens (referred to as PSB∩PISB CIS genes) across the 26 breast tumors analyzed. In each tumor, PSB∩PISB CIS genes containing SB insertions are depicted as blue boxes. The histograms show the total number of PSB∩PISB CIS genes with insertions per each tumor. Red horizontal lines represent the median of PSB∩PISB CIS genes with insertions per PSB (left) and PISB (right) tumors, respectively. **(c)** Scattered plot showing the correlation between the frequency of PSB and PISB breast tumors with insertions in each single PSB∩PISB CIS gene (n=19). *R*, Pearson correlation coefficient. *P* value was calculated by Pearson's correlation test. **(d)** Overlap between PSB (n=287) and PISB (n=665) CIS genes identified in skin tumors. *P* value was calculated using a two-by-two contingency table and Fisher's exact test. **(e)** Distribution of overlapping skin CIS genes (n=143) between PSB and PISB screens (referred to as PSB∩PISB CIS genes) across the 125 skin tumors analyzed. In each tumor, PSB∩PISB CIS genes containing SB insertions are depicted as blue boxes. The histograms show the total number of PSB∩PISB CIS genes with insertions per each tumor. Red horizontal lines represent the median of PSB∩PISB CIS genes with insertions per PSB (left) and PISB (right) tumors, respectively. **(f)** Scattered plot showing the correlation between the frequency of PSB and PISB skin tumors with insertions in each single PSB∩PISB CIS gene (n=143)

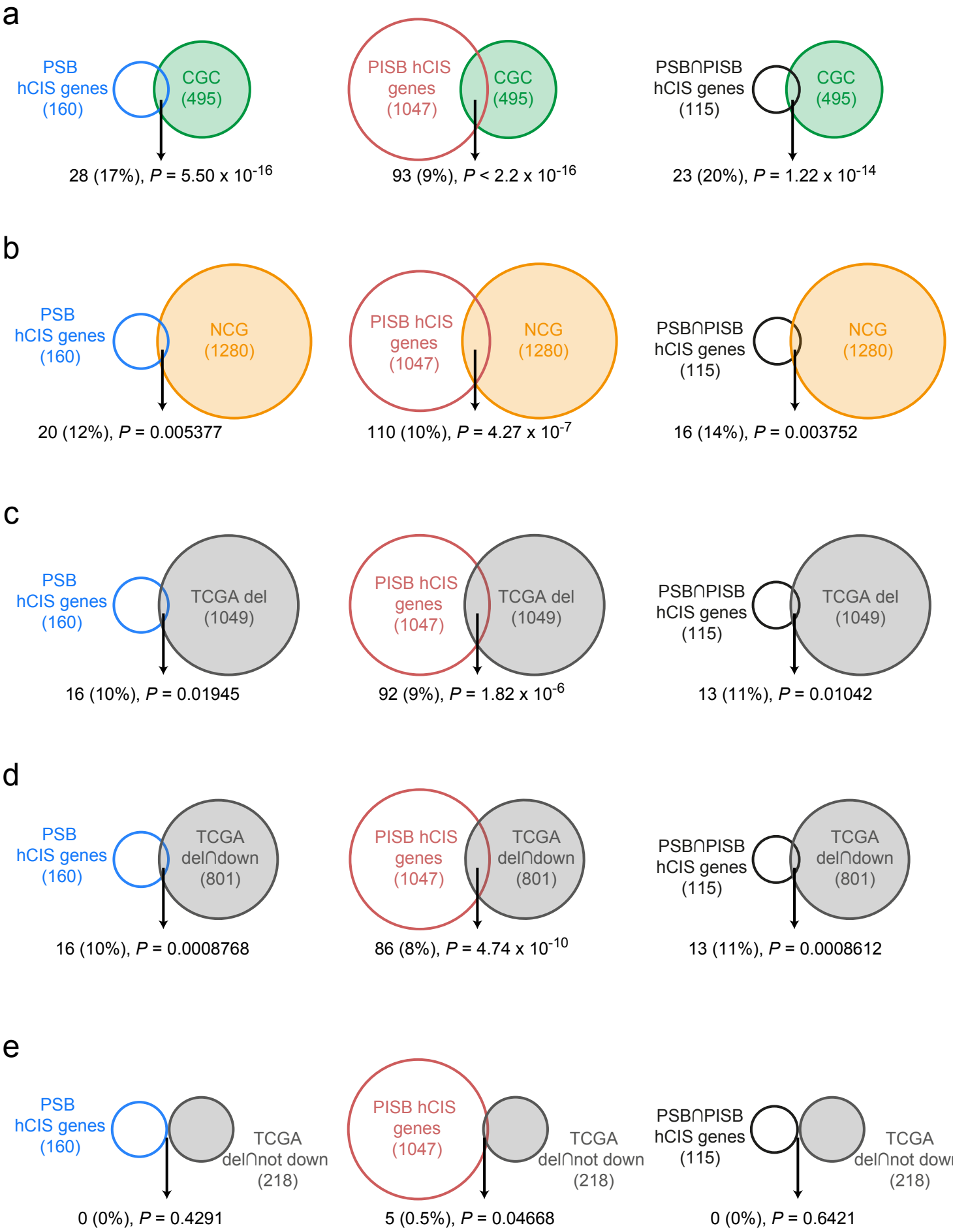

Supplementary Figure 4

Supplementary Figure 4. Cross-species comparisons of mouse hCIS and human cancer genes. Overlap of PSB, PISB and PSB∩PISB hCIS genes with **(a)** genes listed in the Cancer Gene Census database, **(b)** candidate cancer genes registered in the Network of Cancer Genes (NCG) repository, **(c)** genes frequently deleted (> 4% of samples) in human prostate cancers available through The Cancer Genome Atlas (TCGA), **(d)** genes in **c** which are also significantly downregulated and **(e)** genes in **c** which are not significantly downregulated. The number of genes included in each group/dataset is indicated. Human genes whose mouse orthologues map to chromosomes 14 and 19 were not included in the analysis. Percentages in parenthesis represent the proportion of PSB, PISB or PSB∩PISB hCIS overlapping with each of the three datasets. *P* values were calculated using a two-by-two contingency table and Fisher's exact test.

AFF4 Chr11:53350833-53421830;+

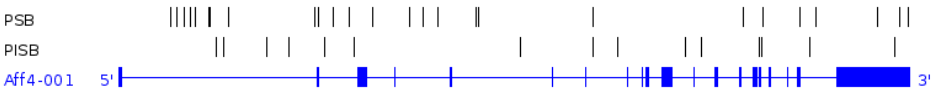

AKAP13 Chr7:75455534-75754609;+

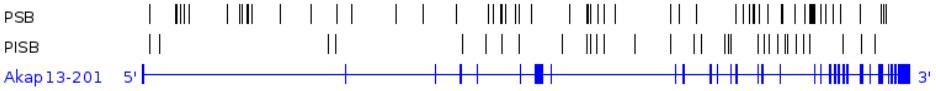

AP4S1 Chr12:51690966-51738939;+

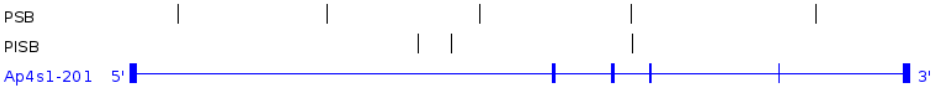

ARID1A Chr4:133679008-133756769;-

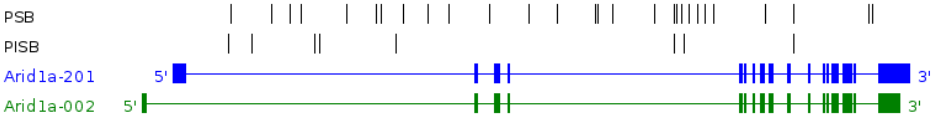

ARID1B Chr17:4994332-5347656;+

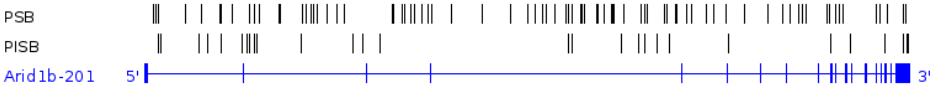

ARIH1 Chr9:59388258-59486618;-

ARL15 Chr13:113794505-114157461;+

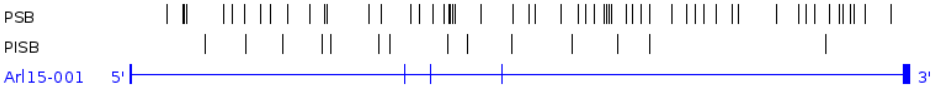

ASH1L Chr3:88950622-89079375;+

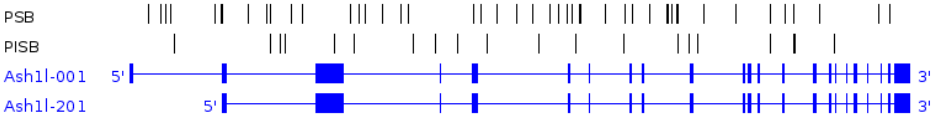

Supplementary Figure 5

ATP2A2 Chr5:122453513-122502225;-

BPTF Chr11:107033081-107132127;-

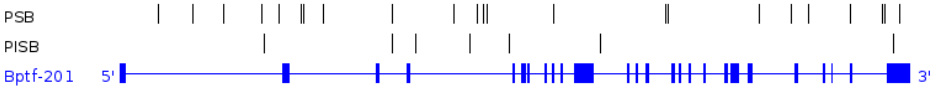

BRD4 Chr17:32196274-32284722;-

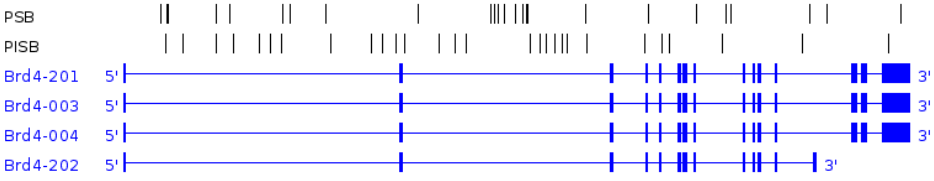

CDC42 Chr4:137319696-137357720;-

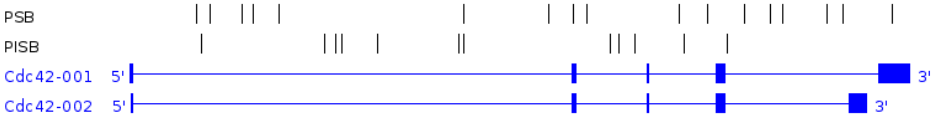

CELF2 Chr2:6539694-7509563;-

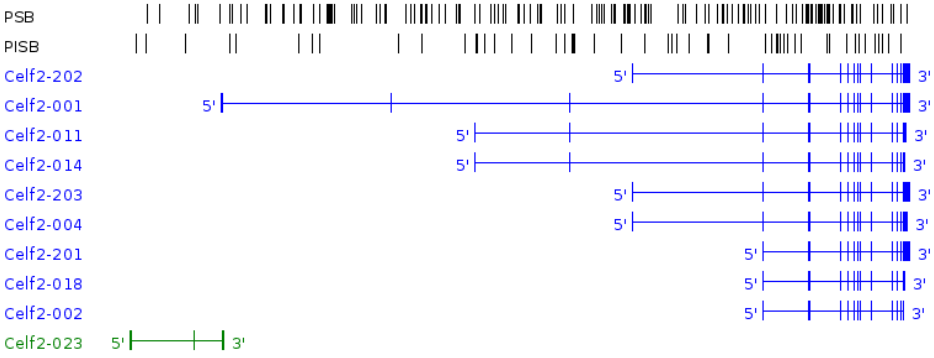

CHD2 Chr7:73426638-73541830;-

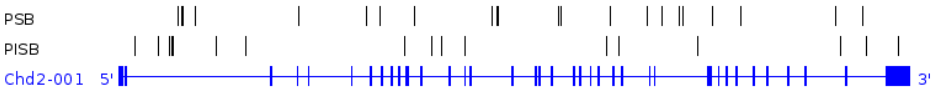

CHD9 Chr8:90828352-91054516;+

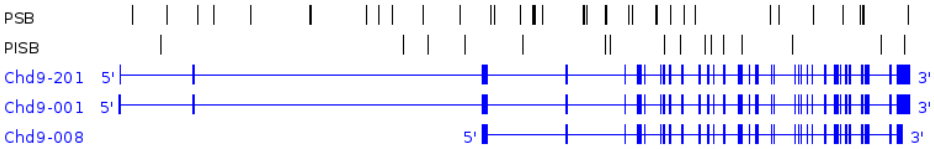

CLINT1 Chr11:45852051-45910625;+

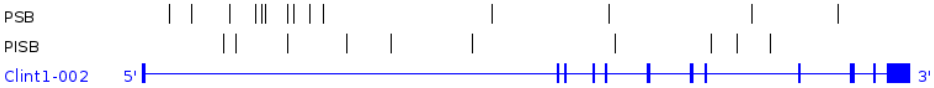

CLTC Chr11:86694351-86757565;-

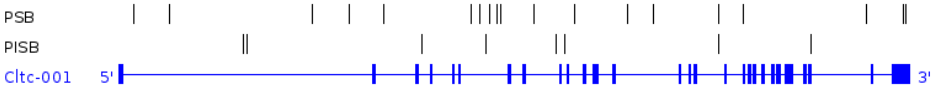

CNOT1 Chr8:95719451-95807464;-

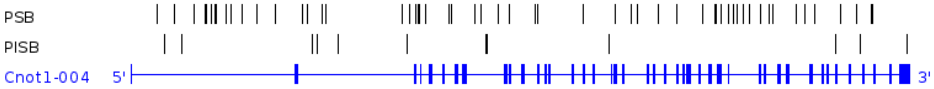

CNOT6L Chr5:96070333-96164171;-

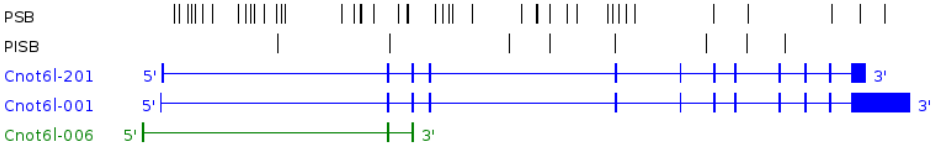

CREBBP Chr16:4081328-4213997;-

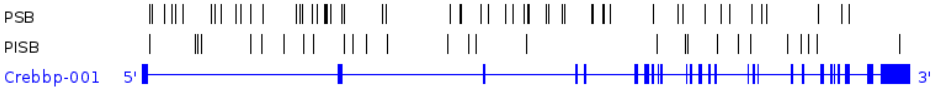

MIA2 Chr12:59095799-59109130;+

CTCF Chr8:105636568-105682922;+

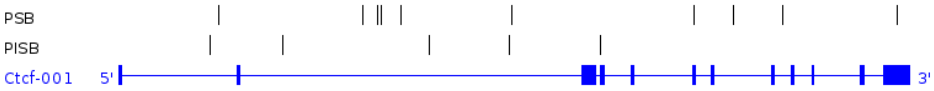

CTNNA1 Chr18:35118888-35254773;+

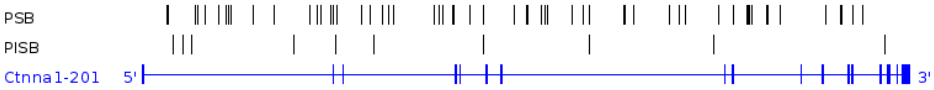

CTNND1 Chr2:84600071-84650765;-

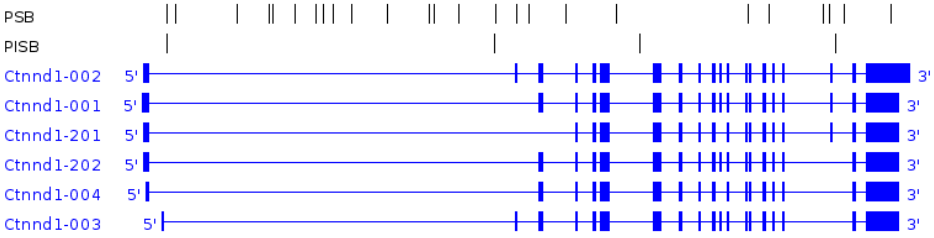

CUL3 Chr1:80264923-80340480;-

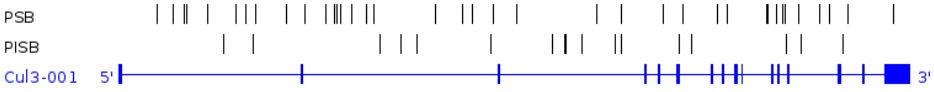

DDX3Y ChrY:1260771-1286629;-

DDX6 Chr9:44604892-44640731;+

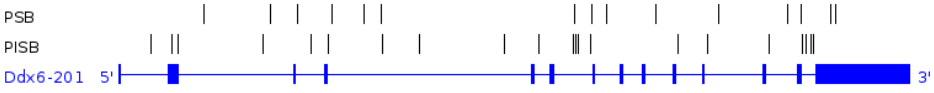

DYRK1A Chr16:94570010-94695517;+

ELL2 Chr13:75707484-75772356;+

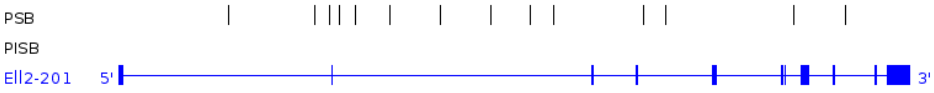

EPB41 Chr4:131923413-132075321;-

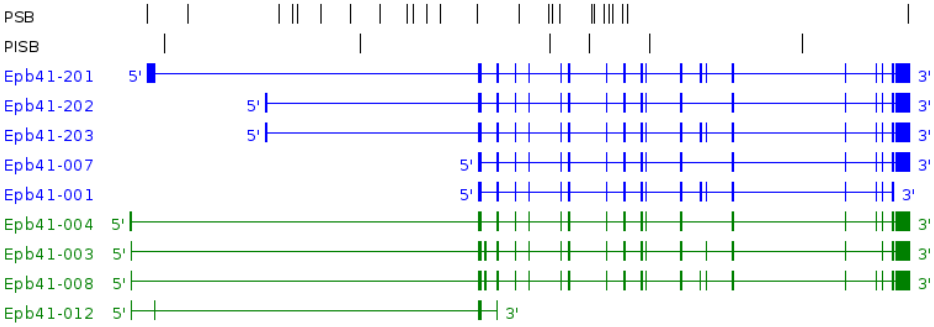

EPC1 Chr18:6435951-6516108;-

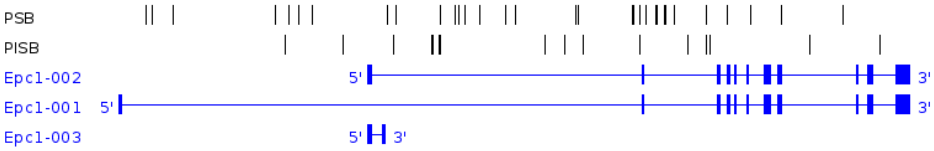

ERBIN Chr13:103818787-103920514;-

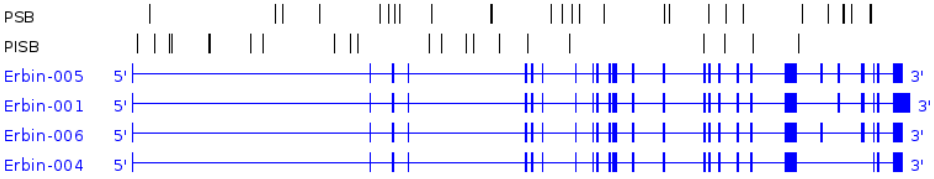

ETL4 Chr2:19909780-20810713;+

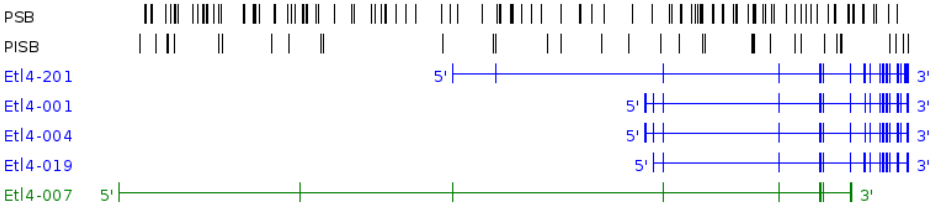

ETV6 Chr6:134035700-134270158;+

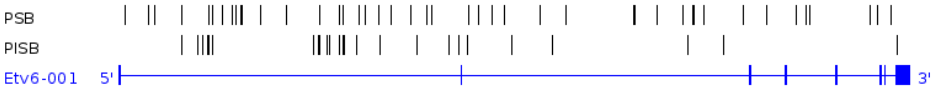

FCHO2 Chr13:98723407-98815449;-

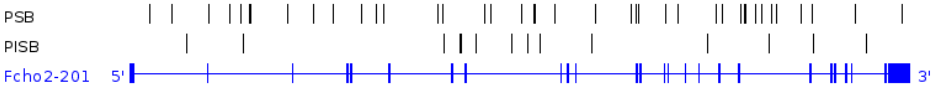

FCHSD2 Chr7:101092863-101284405;+

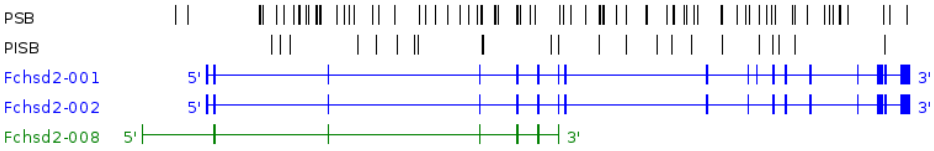

FOXP1 Chr6:98925338-99522721;-

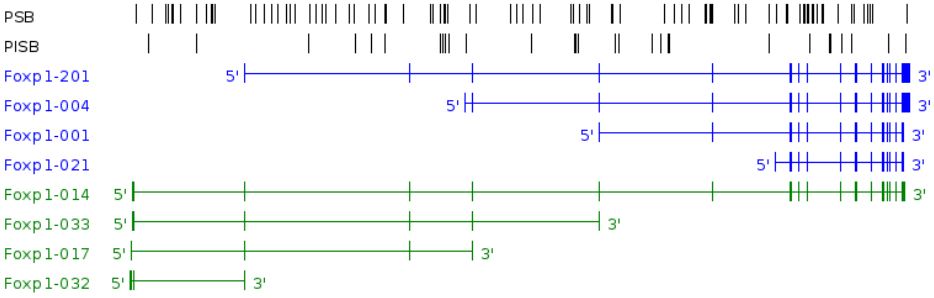

FUBP1 Chr3:152210422-152236826;+

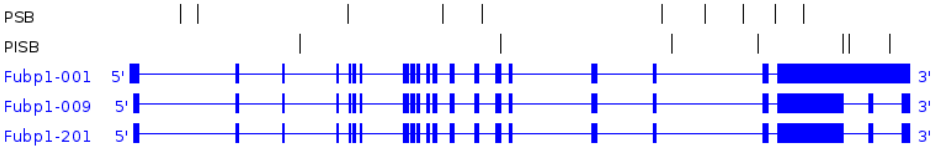

GNB1 Chr4:155491361-155559269;+

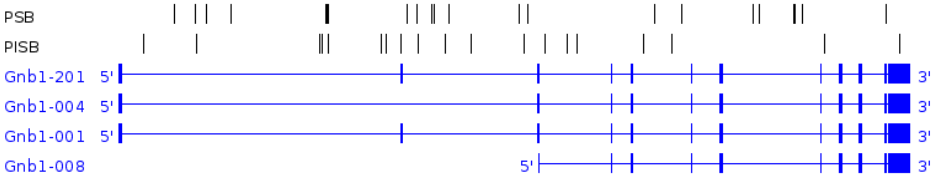

GPBP1 Chr13:111425680-111490111;-

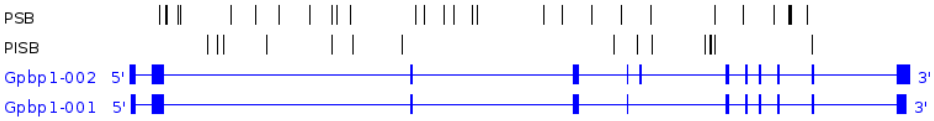

HECTD1 Chr12:51743722-51829536;-

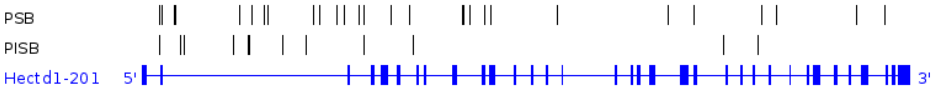

HNRNPM Chr17:33646233-33686860;-

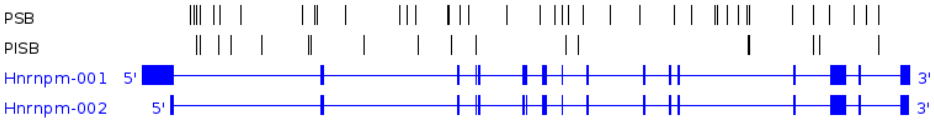

IFT46 Chr9:44767908-44793447;+

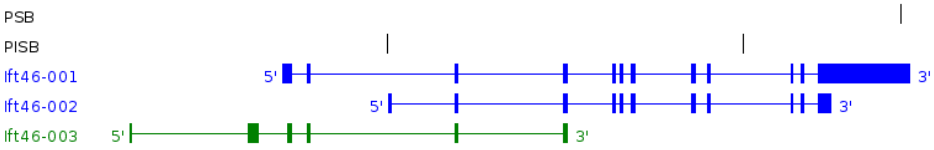

IPO7 Chr7:110018274-110056609;+

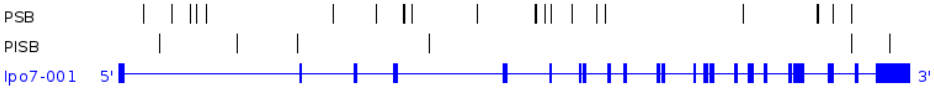

ITSN2 Chr12:4593008-4713950;+

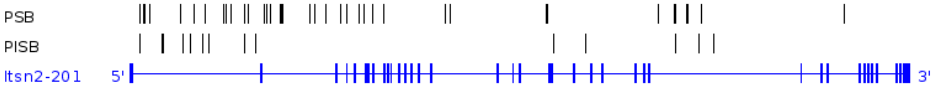

KANSL1 Chr11:104333229-104468861;-

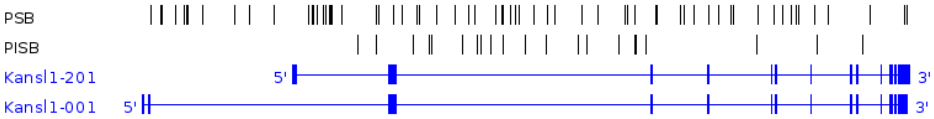

KDM6A ChrX:18162575-18279936;+

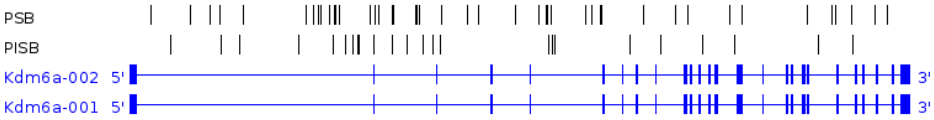

KIF5B Chr18:6201002-6242174;-

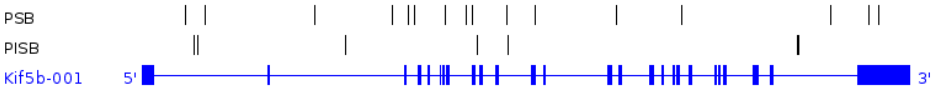

LPP Chr16:24393350-24992576;+

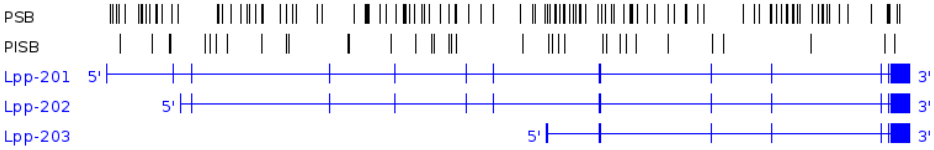

LUC7L2 Chr6:38551334-38609470;+

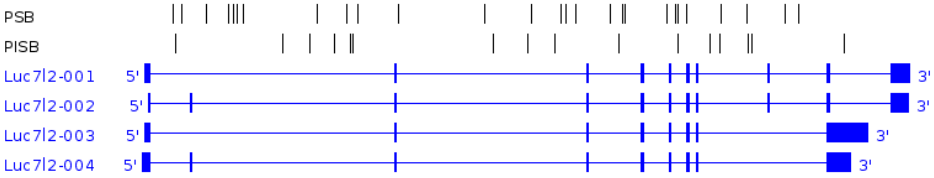

MAGI3 Chr3:104013259-104220374;-

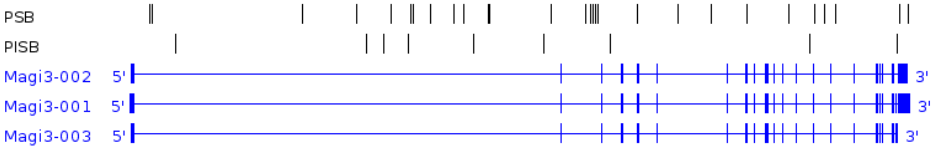

MAP7 Chr10:20148471-20281590;+

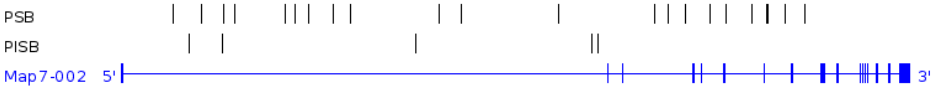

MBNL1 Chr3:60472830-60629750;+

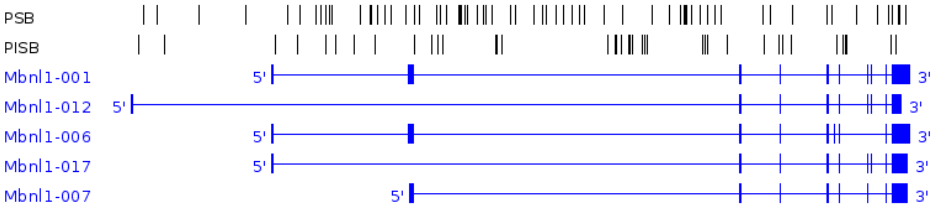

MEIS1 Chr11:18879817-19018985;-

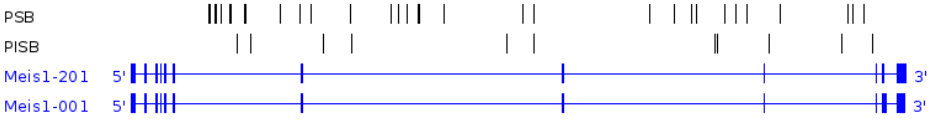

MID1 ChrX:169685199-170005736;+

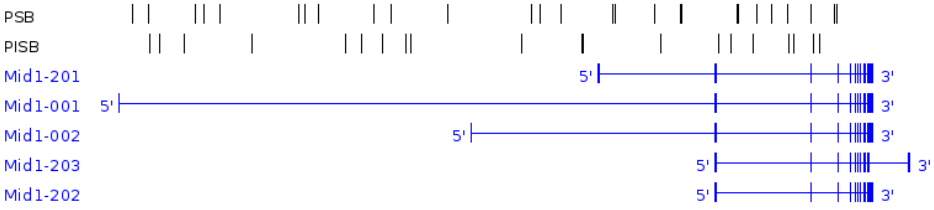

MKL1 Chr15:81012281-81190757;-

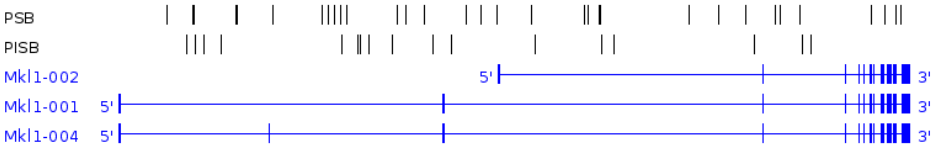

KMT2A Chr9:44803355-44881296;-

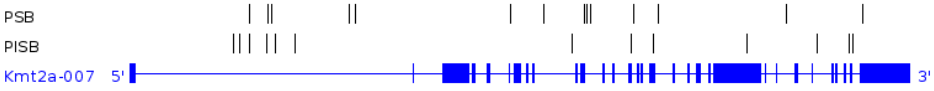

KMT2E Chr5:23434441-23504235;+

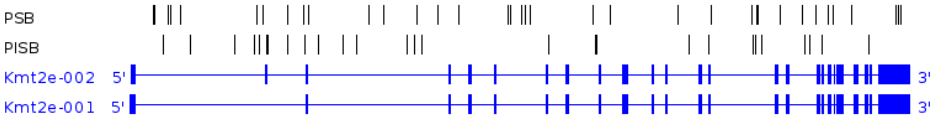

MLLT10 Chr2:18055237-18212388;+

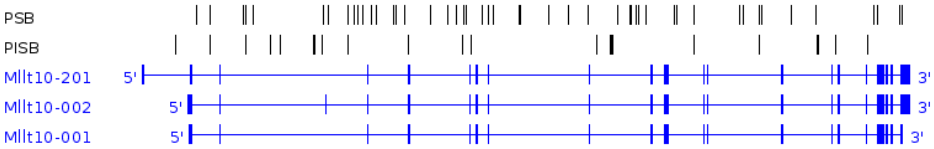

MOB2 Chr7:142008535-142061065;-

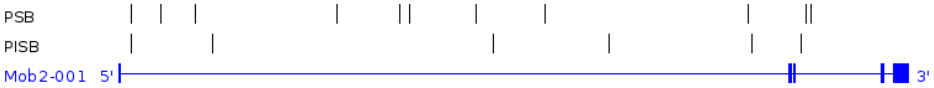

MSI2 Chr11:88339382-88718513;-

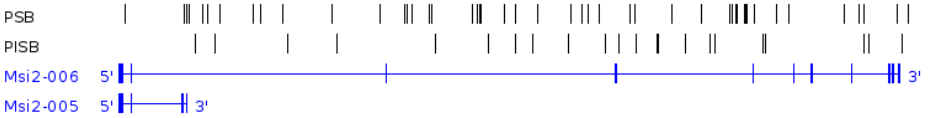

NF1 Chr11:79339693-79581612;+

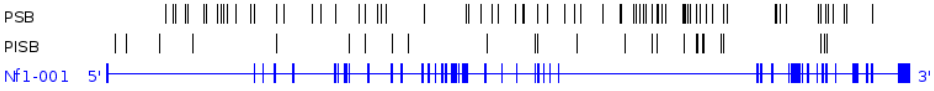

NFIB Chr4:82290173-82705750;-

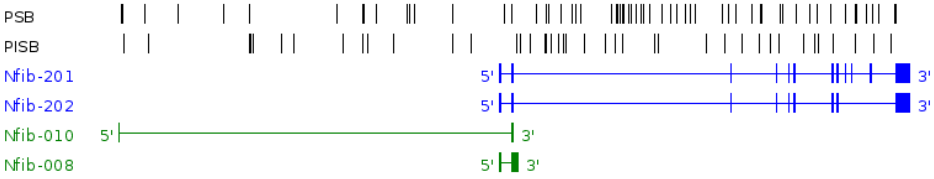

NIPBL Chr15:8291225-8444463;-

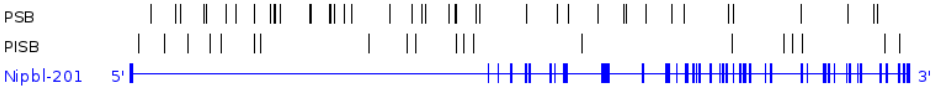

NRIP1 Chr16:76287400-76373827;-

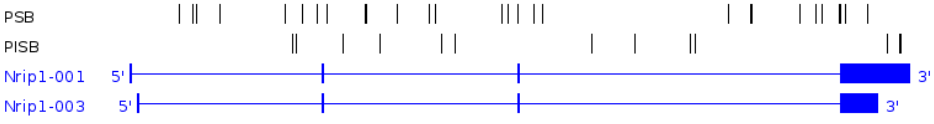

NSD1 Chr13:55209782-55318325;+

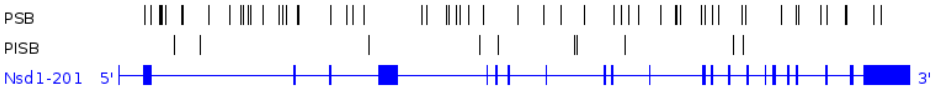

PAK2 Chr16:32016290-32079342;-

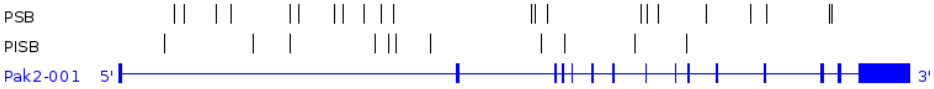

PAN3 Chr5:147430161-147548502;+

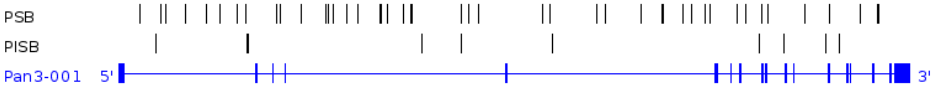

PARD3 Chr8:127063893-127612286;+

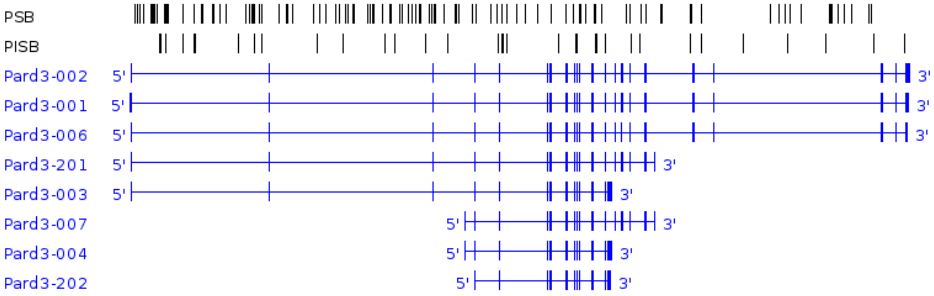

PBX1 Chr1:168119364-168432270;-

PELI1 Chr11:21091291-21150323;+

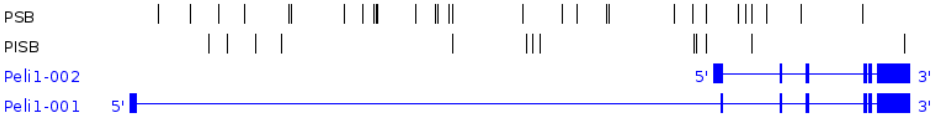

PHIP Chr9:82866159-82975516;-

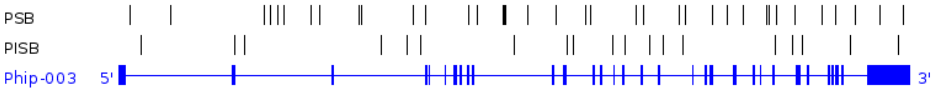

PIK3R1 Chr13:101680563-101768217;-

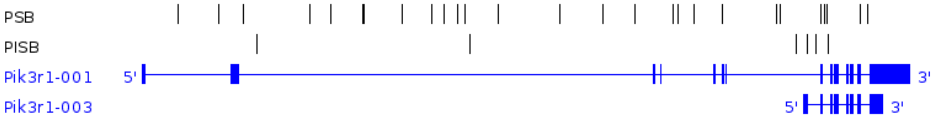

PPP1R12A Chr10:108162400-108277575;+

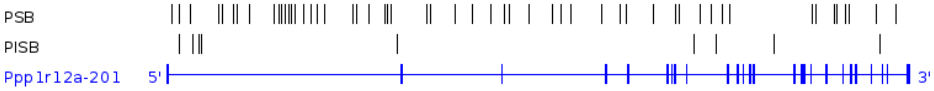

PTBP3 Chr4:59471868-59549364;-

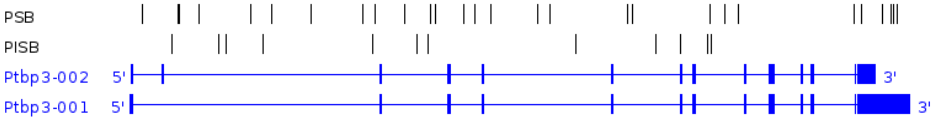

PTPRC Chr1:138062861-138175708;-

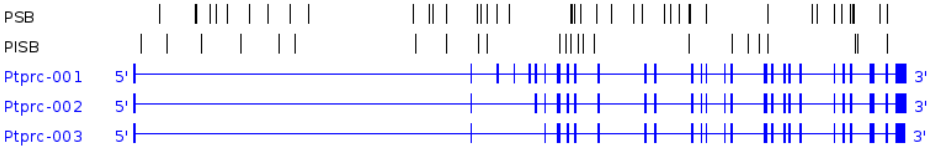

PUM1 Chr4:130663321-130781564;+

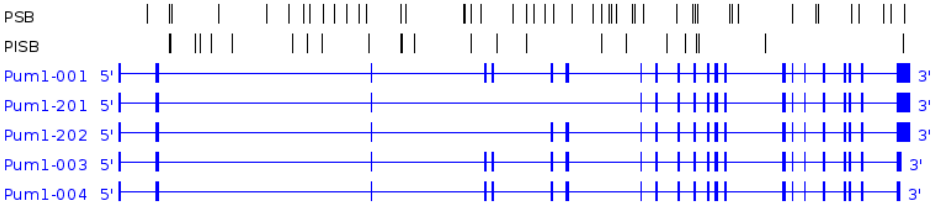

RAB10 Chr12:3247430-3309969;-

RASA1 Chr13:85214780-85289029;-

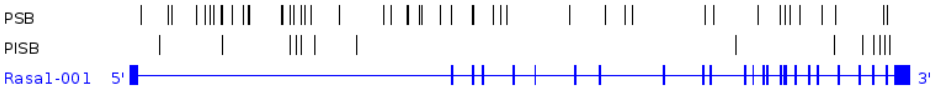

RBM39 Chr2:156147239-156180238;-

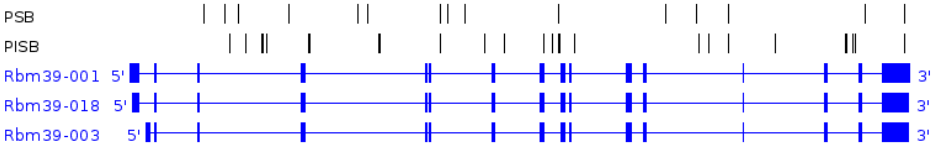

RBM6 Chr9:107773559-107873237;-

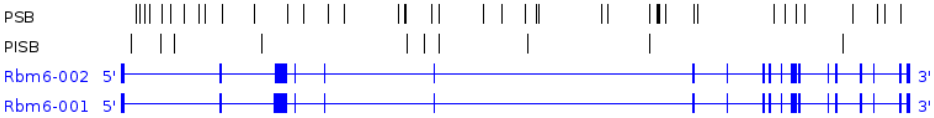

RHOA Chr9:108306129-108337934;+

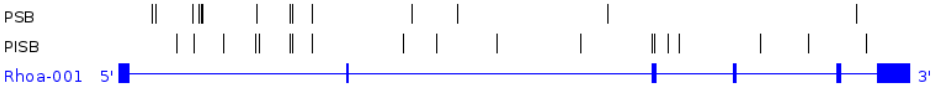

RRBP1 Chr2:143947395-144011263;-

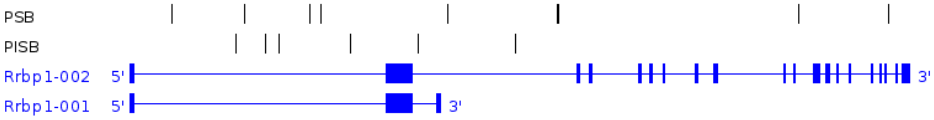

SEC63 Chr10:42761496-42832514;+

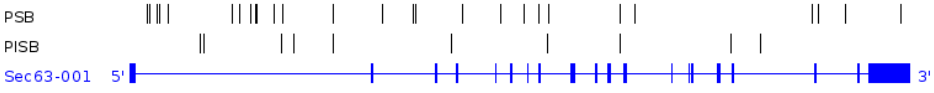

SF3B1 Chr1:54985169-55027481;-

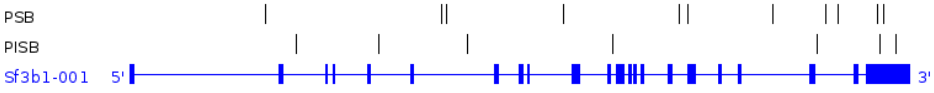

SFPQ Chr4:127021324-127037013;+

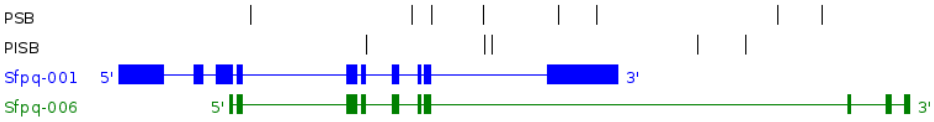

SNX2 Chr18:53176365-53220860;+

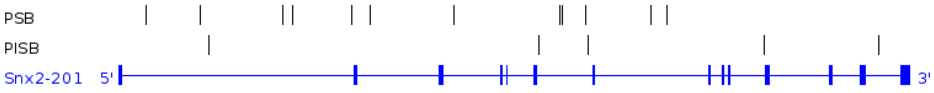

SP3 Chr2:72936427-72980446;-

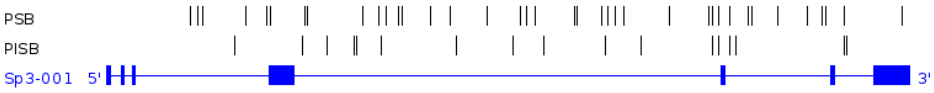

SRSF4 Chr4:131873617-131901706;+

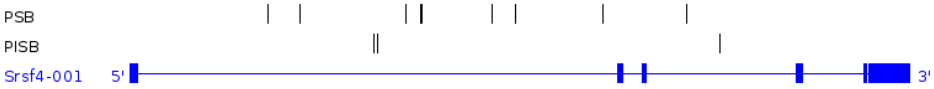

ST5 Chr7:109523911-109703605;-

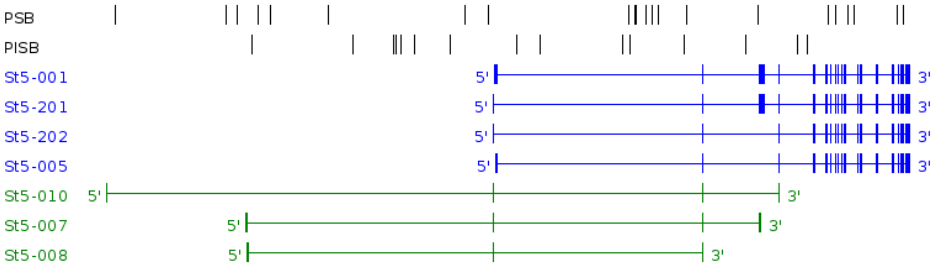

TBL1X ChrX:77511013-77662983;+

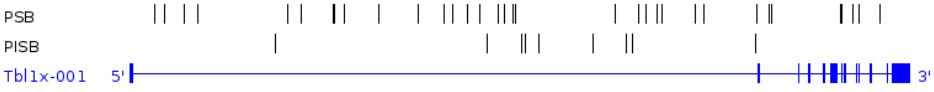

TBL1XR1 Chr3:22076652-22216594;+

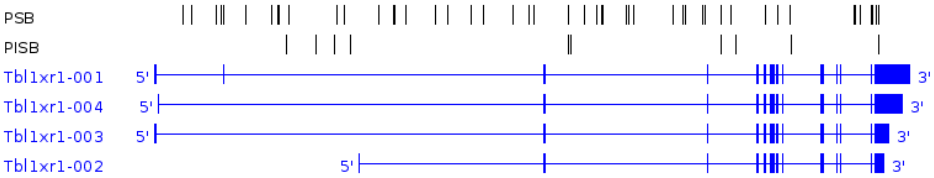

TLK1 Chr2:70712407-70825728;-

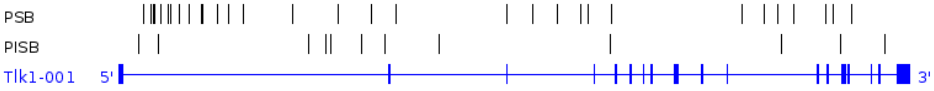

TNPO1 Chr13:98839019-98926384;-

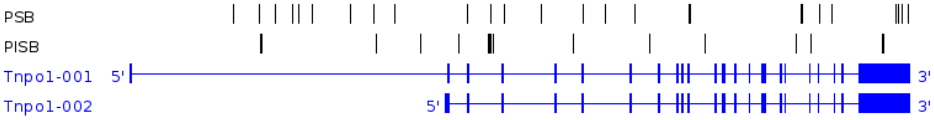

TNRC6B Chr15:80711319-80941086;+

TRIP12 Chr1:84721189-84840516;-

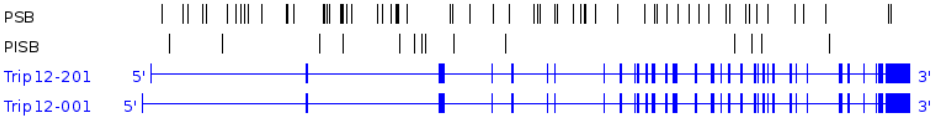

UBA1Y ChrY:818649-844224;+

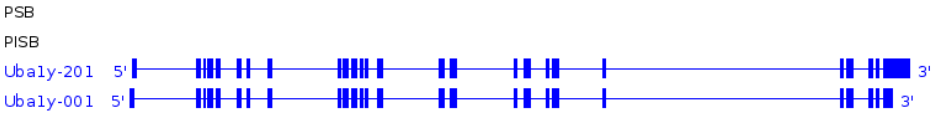

UBE2D3 Chr3:135438149-135468198;+

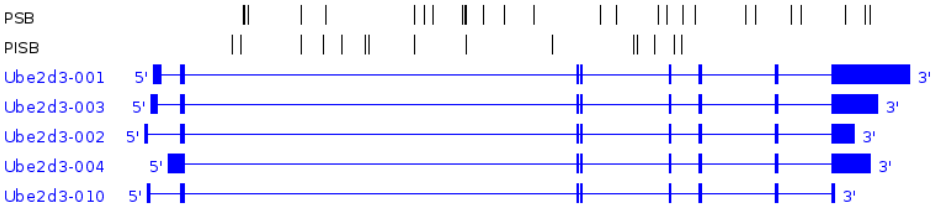

UBE2N Chr10:95515162-95545658;+

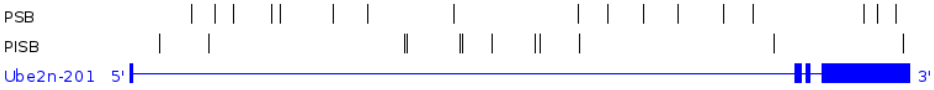

UBE3A Chr7:59228750-59311536;+

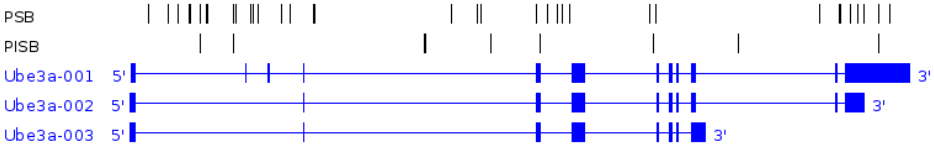

USP7 Chr16:8689595-8792308;-

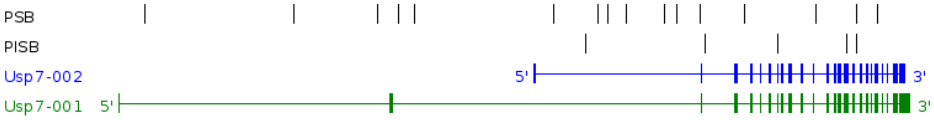

USP9Y ChrY:1298961-1459782;-

UTY ChrY:1096861-1245759;-

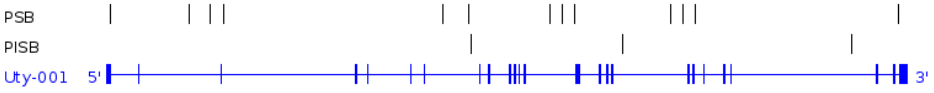

WAC Chr18:7868832-7973547;+

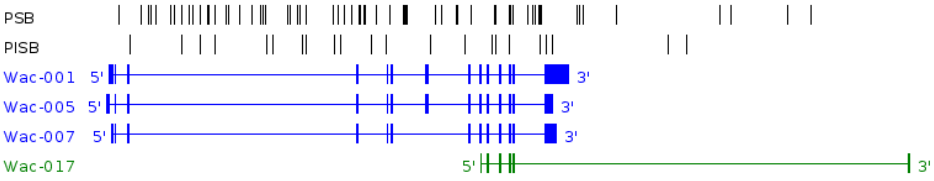

WDFY3 Chr5:101832956-102069921;-

YTHDF2 Chr4:132184912-132212303;-

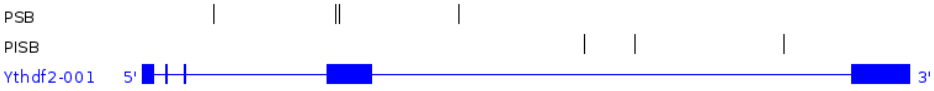

YTHDF3 Chr3:16183212-16217037;+

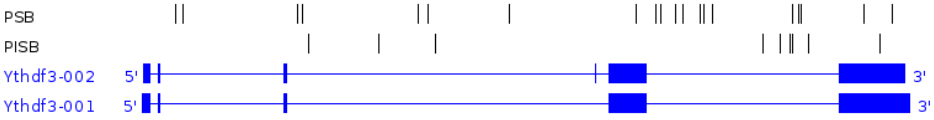

YWHAE Chr11:75732869-75765845;+

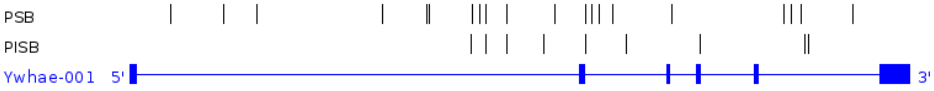

YY1 Chr12:108792973-108816632;+

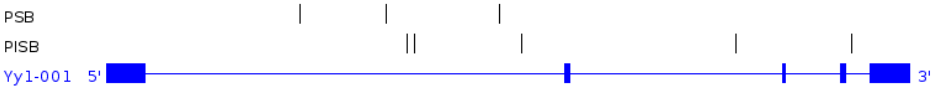

ZBTB20 Chr16:42875881-43642602;+

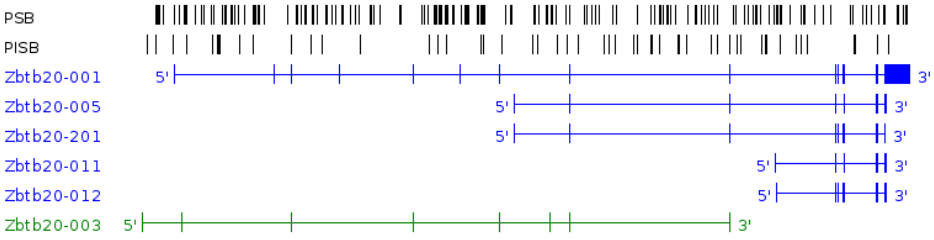

ZFAND3 Chr17:30005087-30210019;+

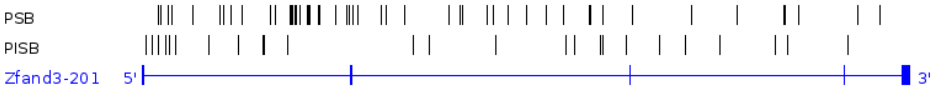

ZFP148 Chr16:33380775-33503903;+

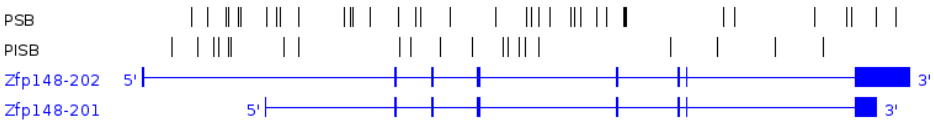

ZFP292 Chr4:34803113-34882960;-

ZFY1 ChrY:725128-797409;-

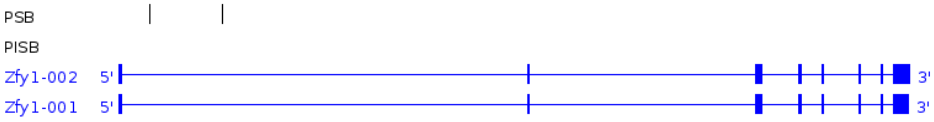

ZFY2 ChrY:2106015-2170409;-

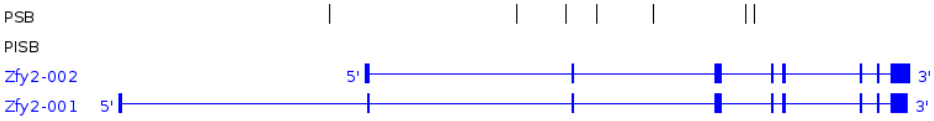

2010111I01RIK Chr13:63014934-63326096;+

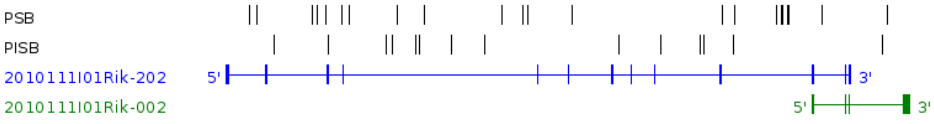

Supplementary Figure 5. Transposon integration pattern across the PSB∩PISB CIS genes in PSB and PISB prostate tumors. Only the transposon insertions falling in the genes nearest to the center of each CIS peak are represented. Only the consensus CDS (CCDS) transcripts are shown (blue) unless these cover less than 98% of the annotated gene length, in which case non-CCDS transcripts are also depicted (green). Genes without insertions correspond to the gene closest to the center of an intergenic CIS.

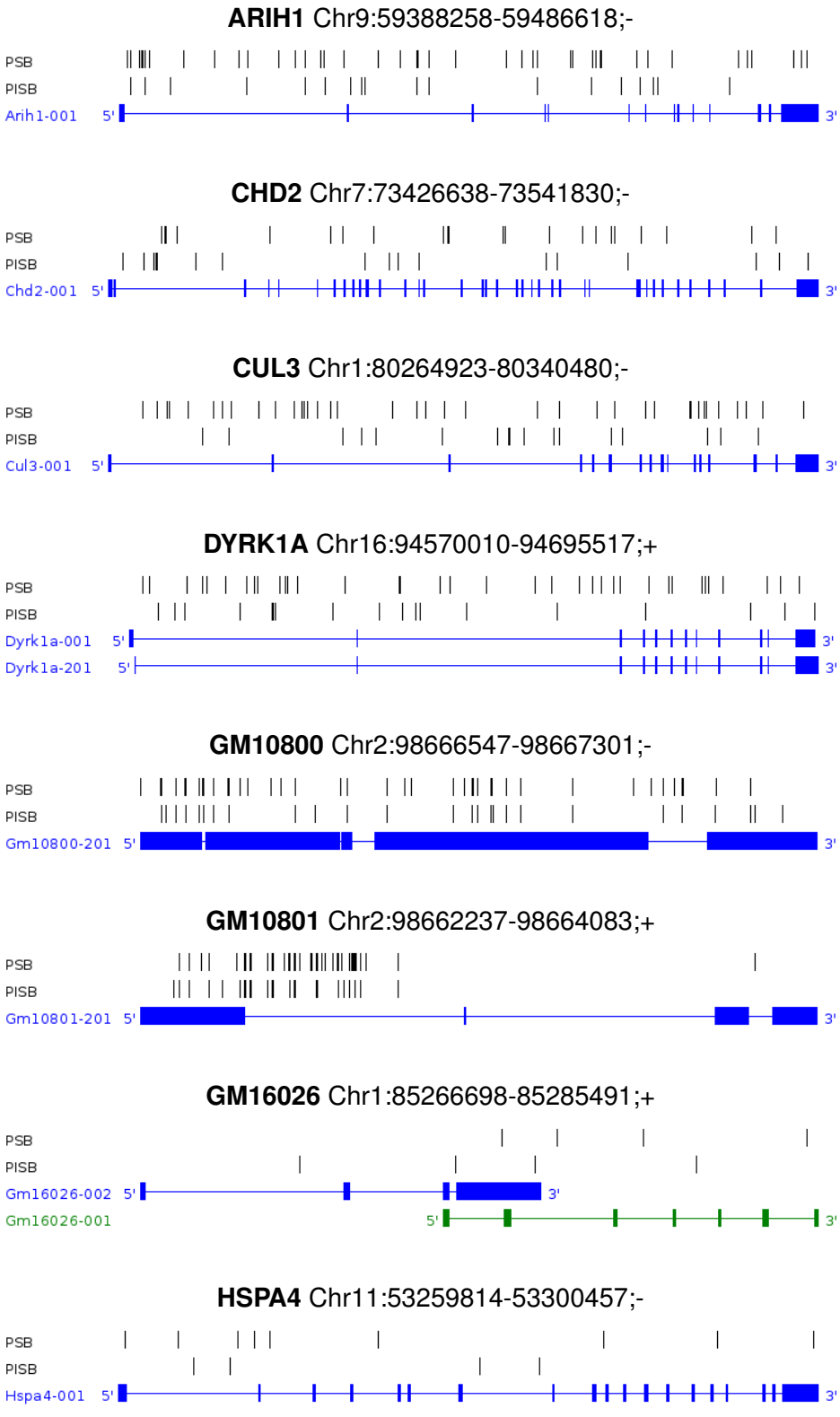

Supplementary Figure 6

KANSL1 Chr11:104333229-104468861;-

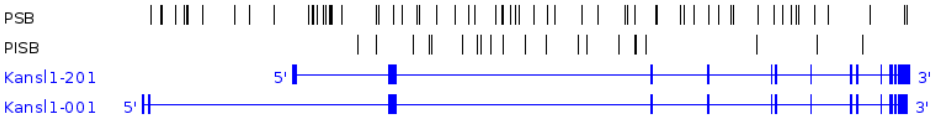

NF1 Chr11:79339693-79581612;+

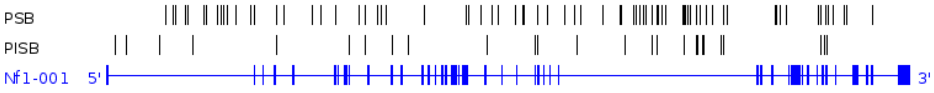

OSMR Chr15:6813577-6874969;-

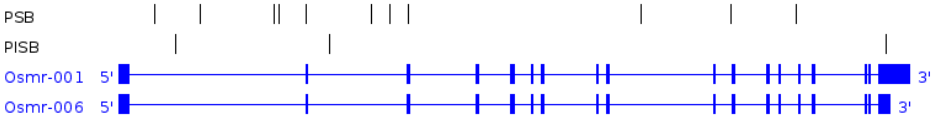

PCSK7 Chr9:45906497-45929726;+

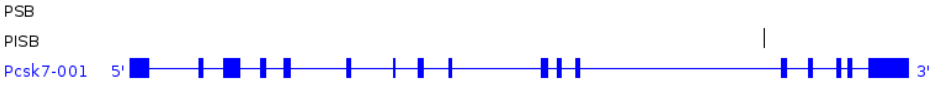

PIAS1 Chr9:62878368-62987924;-

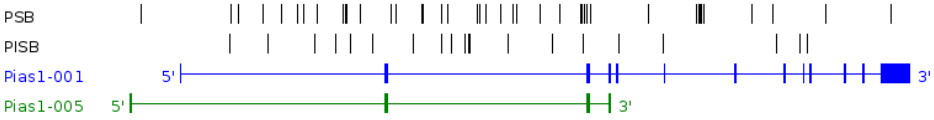

PRL2C2 Chr13:12996132-13005383;-

RALGAPB Chr2:158409848-158499253;+

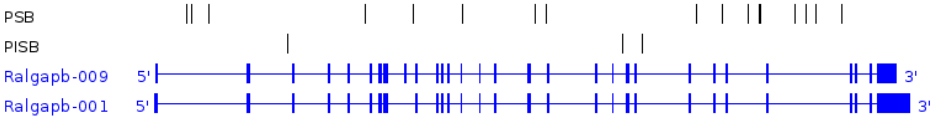

TNRC6B Chr15:80711319-80941086;+

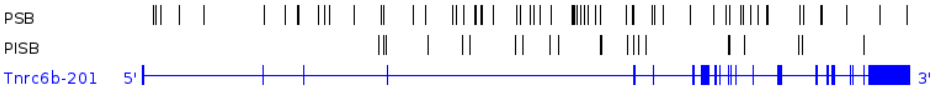

TRP53 Chr11:69580359-69591873;+

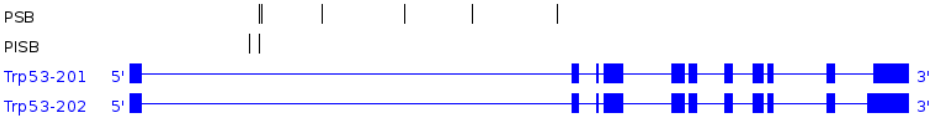

TRPS1 Chr15:50654752-50890463;-

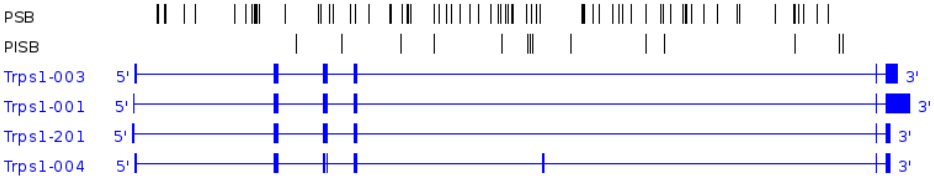

UBA1 ChrX:20658326-20683179;+

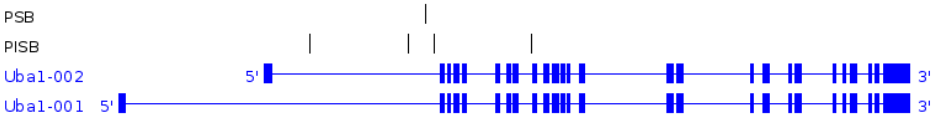

Supplementary Figure 6. Transposon integration pattern across the PSB∩PISB CIS genes in PSB and PISB breast tumors. Only the transposon insertions falling in the genes nearest to the center of each CIS peak are represented. For these genes, only the consensus CDS (CCDS) transcripts are shown (blue) unless these cover less than 98% of the annotated gene length, in which case non-CCDS transcripts are also depicted (green).

ABI1 Chr2:22940073-23040241;-

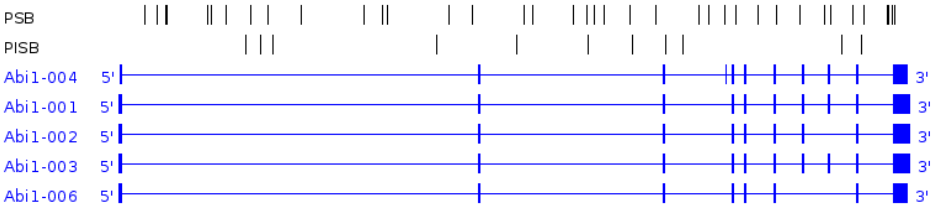

ACTR2 Chr11:20062304-20112913;-

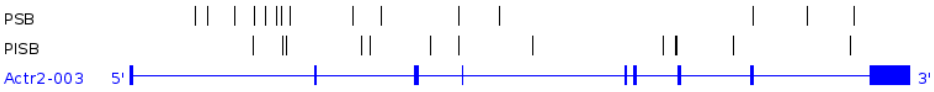

ACTR3 Chr1:125392905-125435727;-

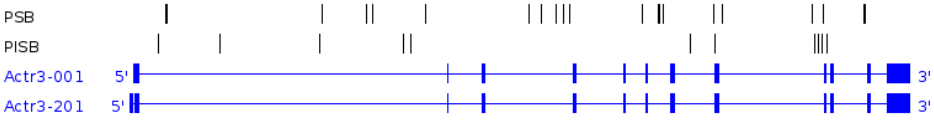

AI314180 Chr4:58798911-58912749;-

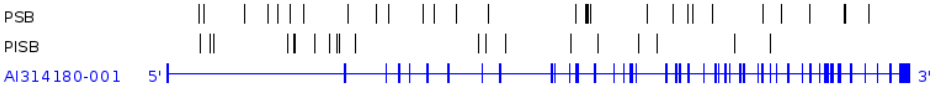

AKAP13 Chr7:75455534-75754609;+

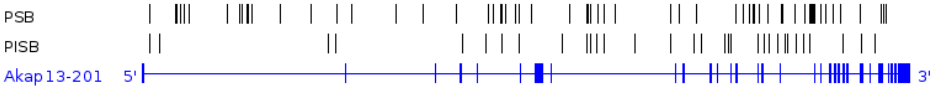

ANKHD1 Chr18:36559987-36665917;+

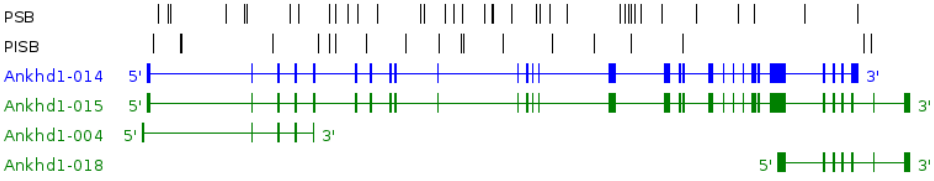

ARIH1 Chr9:59388258-59486618;-

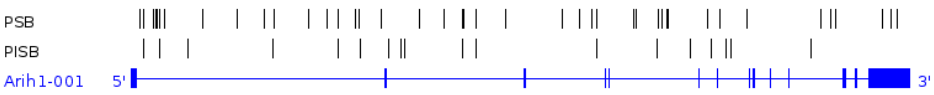

Supplementary Figure 7

ASAP1 Chr15:64086857-64382919;-

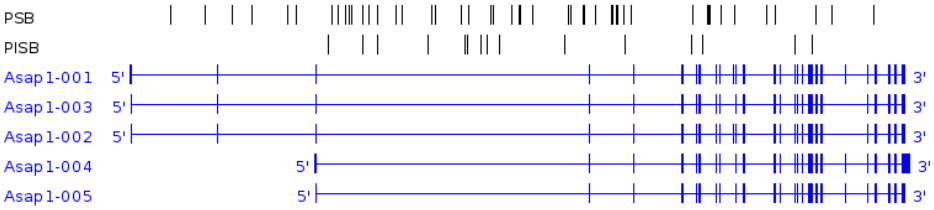

ASH1L Chr3:88950622-89079375;+

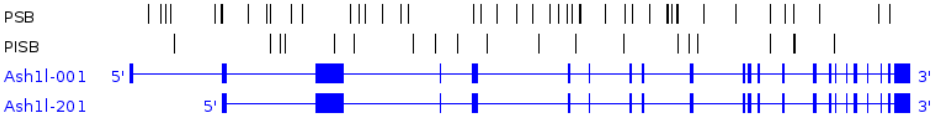

ATAD2B Chr12:4917404-5044047;+

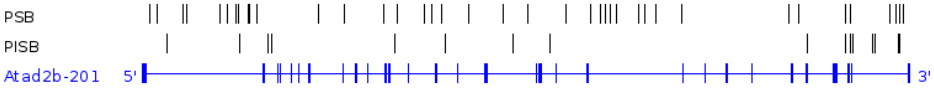

ATXN1 Chr13:45549758-45964991;-

BIRC6 Chr17:74528295-74703356;+

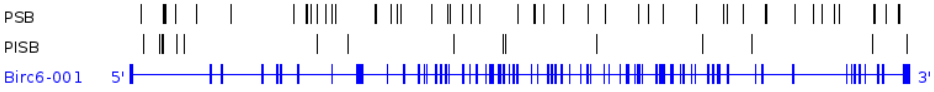

BMPR2 Chr1:59763400-59879014;+

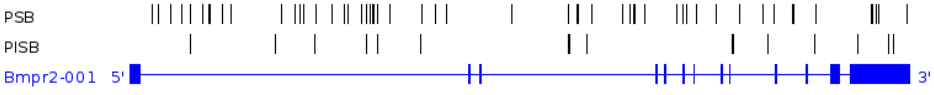

BRD4 Chr17:32196274-32284722;-

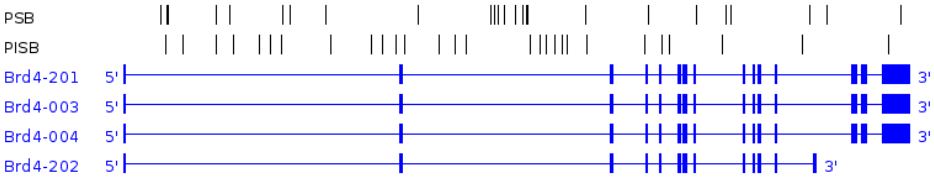

C230088H06RIK Chr4:147018235-147492201;-

CBL Chr9:44142976-44234049;-

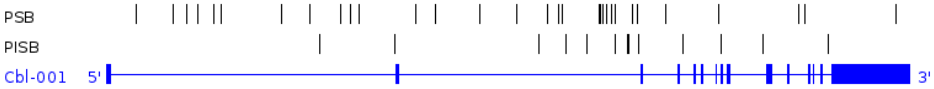

CBLB Chr16:52031549-52208047;+

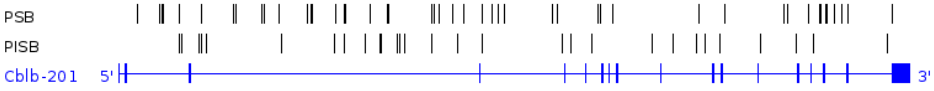

CDC42 Chr4:137319696-137357720;-

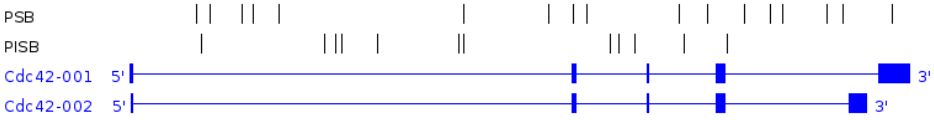

CELF2 Chr2:6539694-7509563;-

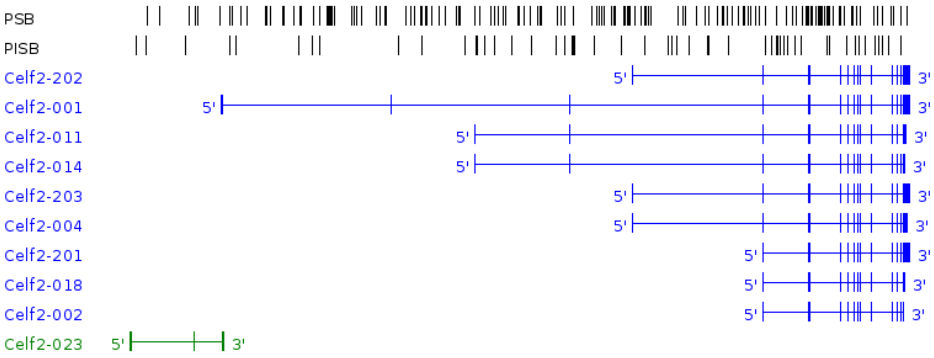

CHD2 Chr7:73426638-73541830;-

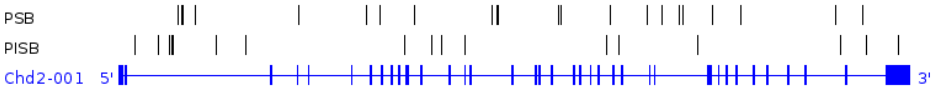

CHL1 Chr6:103510586-103750211;+

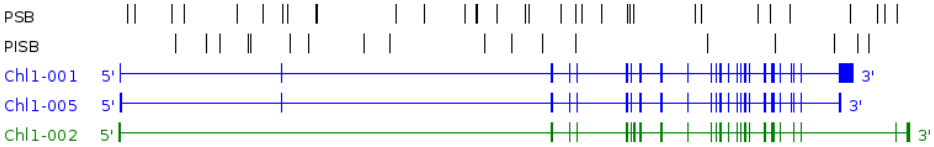

CLDN34D ChrX:76582610-76602924;-

CNOT2 Chr10:116485161-116581511;-

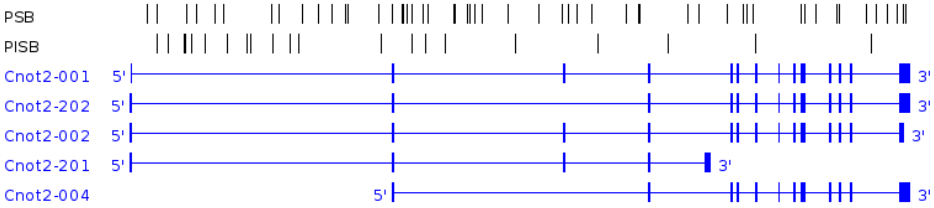

CREBBP Chr16:4081328-4213997;-

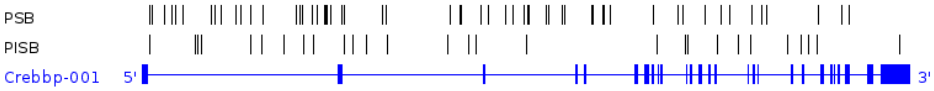

CSNK1G1 Chr9:65908924-66045015;+

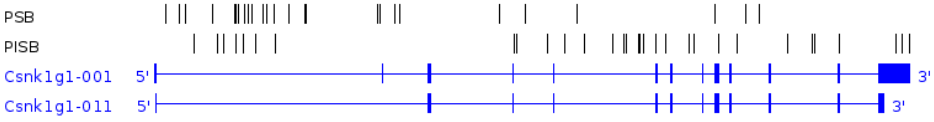

CUL3 Chr1:80264923-80340480;-

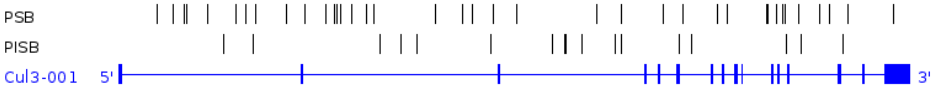

D17WSU92E Chr17:27751232-27820558;-

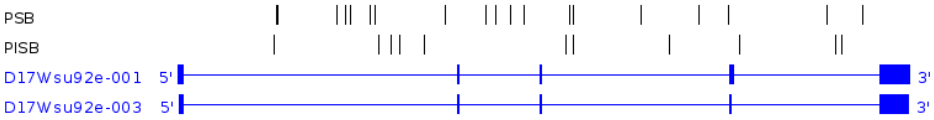

DDX3Y ChrY:1260771-1286629;-

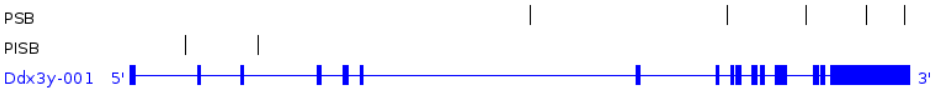

DGKB Chr12:37880705-38633410;+

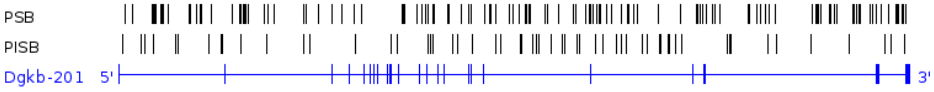

DSC3 Chr18:19960930-20002097;-

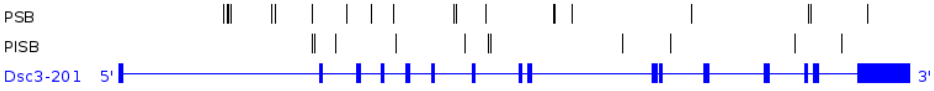

DYRK1A Chr16:94570010-94695517;+

ELMO1 Chr13:20090596-20606528;+

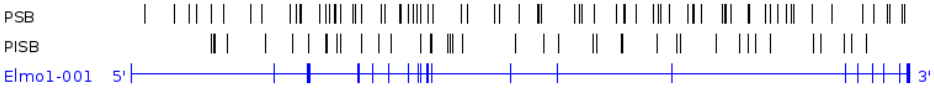

EPC1 Chr18:6435951-6516108;-

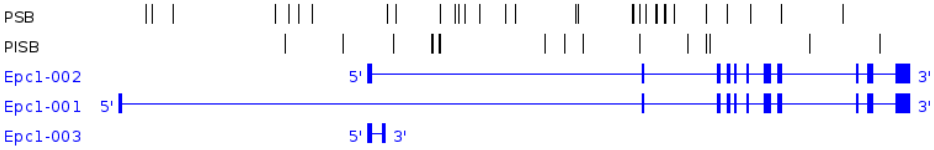

ETV6 Chr6:134035700-134270158;+

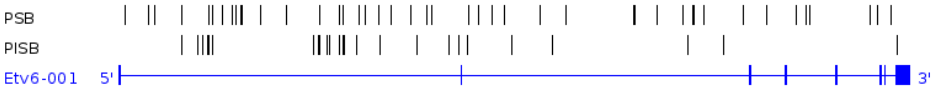

FAM193A Chr5:34369933-34486456;+

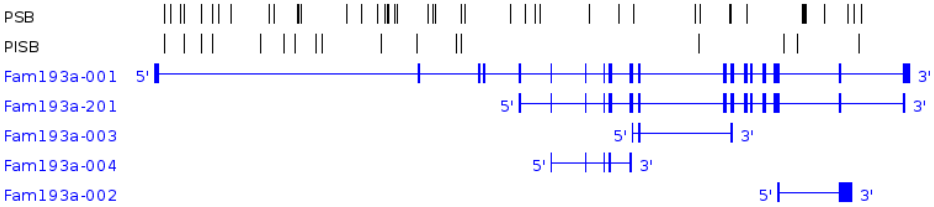

FBXO11 Chr17:87990859-88065291;-

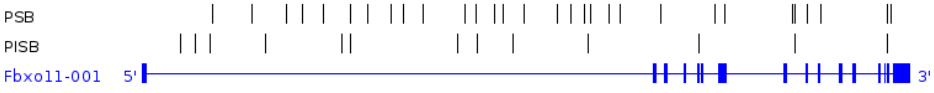

FBXW11 Chr11:32642724-32746816;+

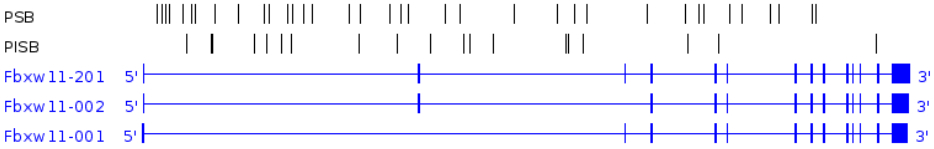

FCHSD2 Chr7:101092863-101284405;+

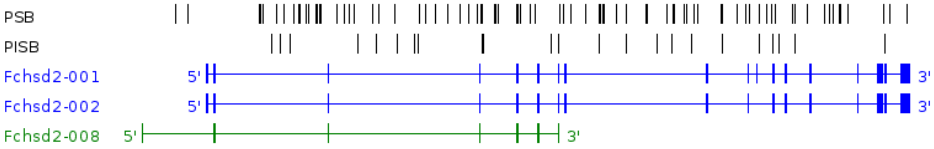

FRYL Chr5:73019987-73256619;-

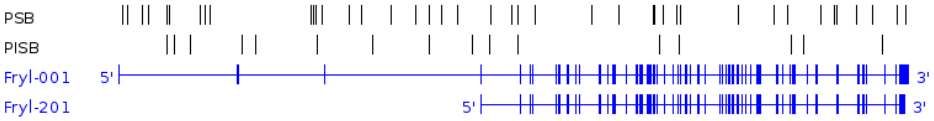

FUT8 Chr12:77238104-77476338;+

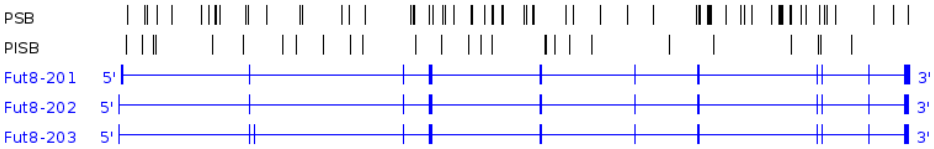

GATAD2B Chr3:90293178-90363407;+

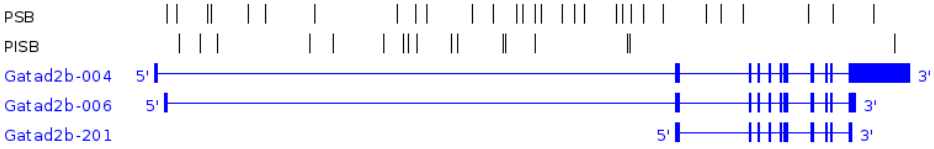

GIGYF2 Chr1:87326998-87450796;+

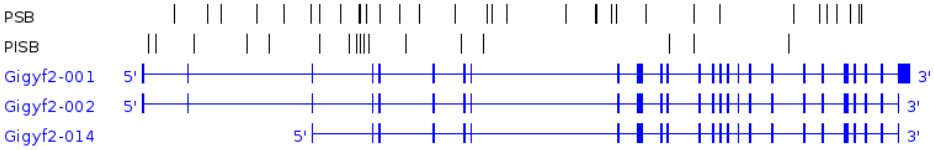

GM10800 Chr2:98666547-98667301;-

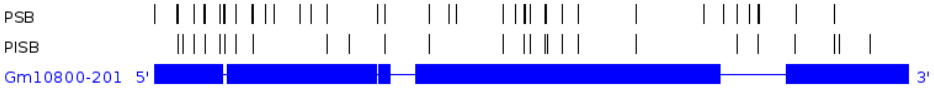

GM10801 Chr2:98662237-98664083;+

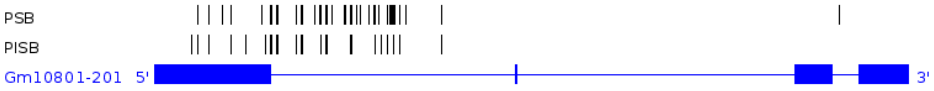

GM16490 Chr18:35770318-35770668;+

GM19710 Chr3:89998760-90021445;+

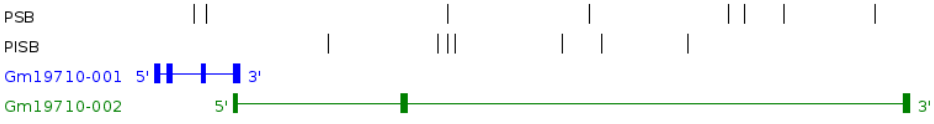

GM20388 Chr8:119910841-124345722;+

GM26870 Chr9:3000282-3038313;-

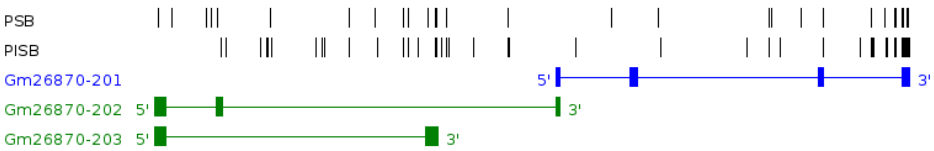

GM28412 ChrY:3909381-3909557;+

GM28507 ChrY:10019064-10019766;-

GM29277 ChrY:206151-207788;+

GM5614 Chr9:35281518-35281835;-

GM9075 Chr12:3082667-3087041;+

GNB1 Chr4:155491361-155559269;+

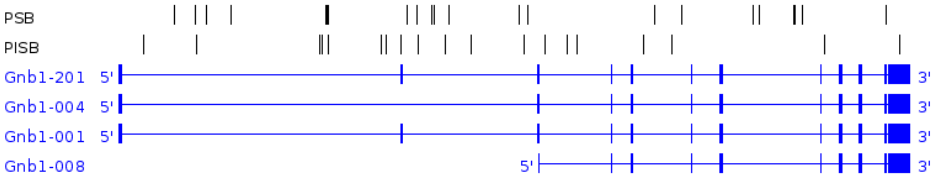

GPATCH8 Chr11:102475915-102556392;-

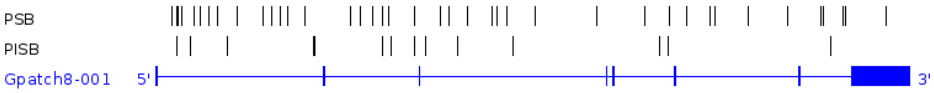

GPBP1 Chr13:111425680-111490111;-

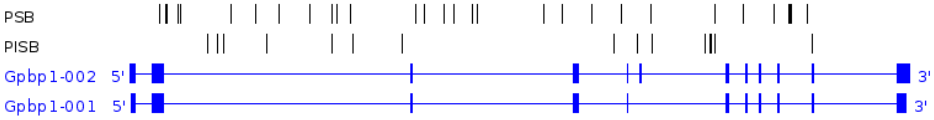

HECTD1 Chr12:51743722-51829536;-

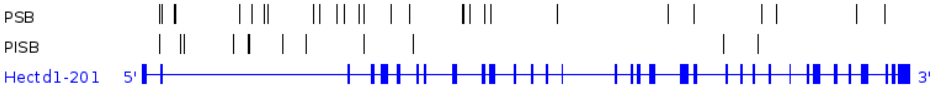

HNRNPM Chr17:33646233-33686860;-

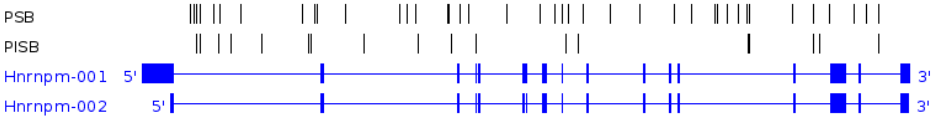

IRF2 Chr8:46739732-46847458;+

ITSN2 Chr12:4593008-4713950;+

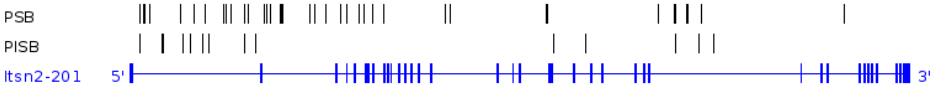

JARID2 Chr13:44729474-44921643;+

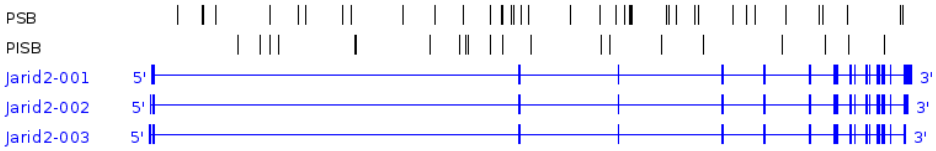

KANSL1 Chr11:104333229-104468861;-

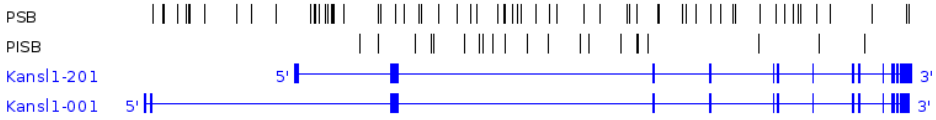

KDM6A ChrX:18162575-18279936;+

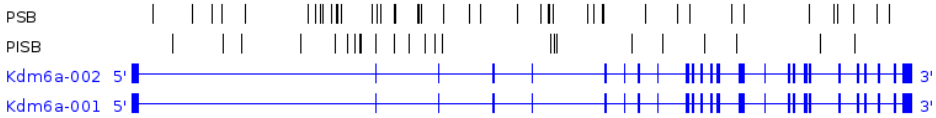

KMT2C Chr5:25271798-25498783;-

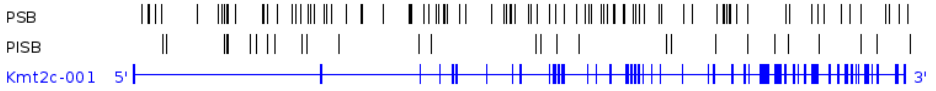

KMT2E Chr5:23434441-23504235;+

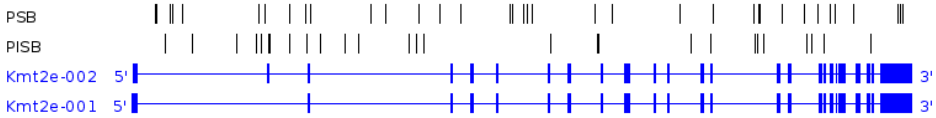

KPNA4 Chr3:69067149-69127113;-

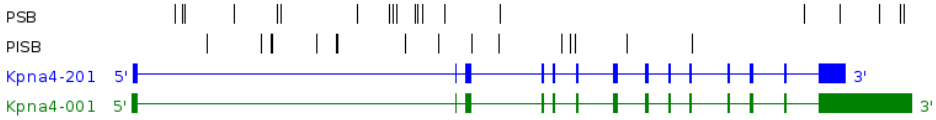

LNPEP Chr17:17527723-17624489;-

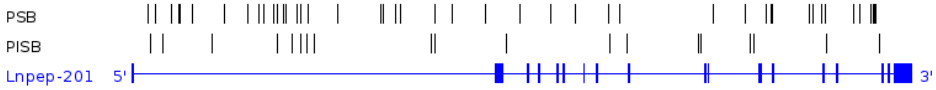

LSM14A Chr7:34344646-34393315;-

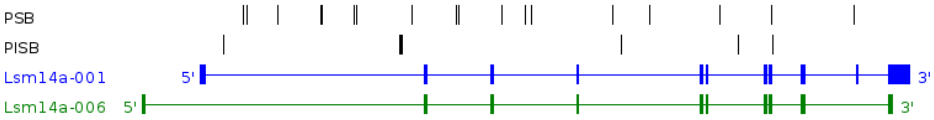

LUC7L2 Chr6:38551334-38609470;+

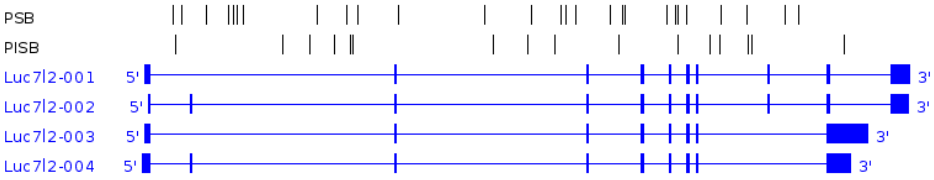

MATR3 Chr18:35562146-35593835;+

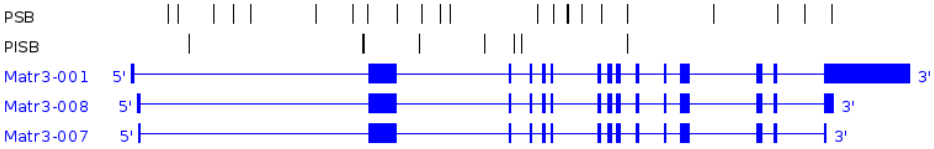

MBNL1 Chr3:60472830-60629750;+

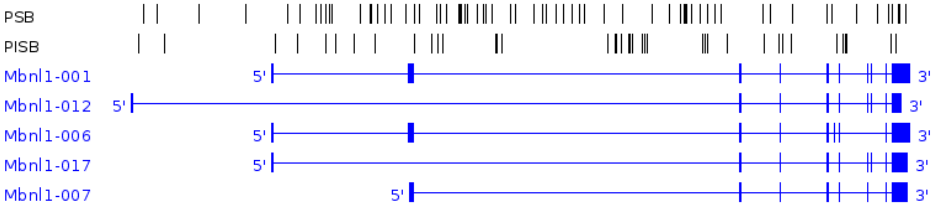

MED13L Chr5:118560679-118765438;+

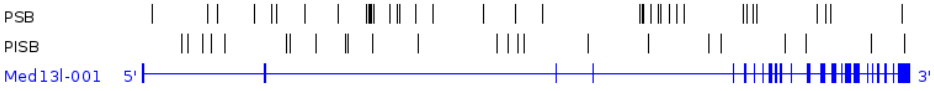

MEF2A Chr7:67231163-67372858;-

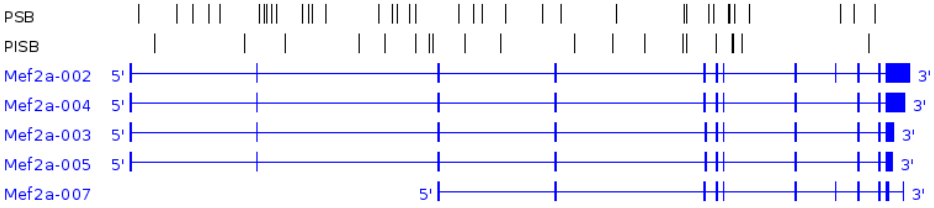

MLLT10 Chr2:18055237-18212388;+

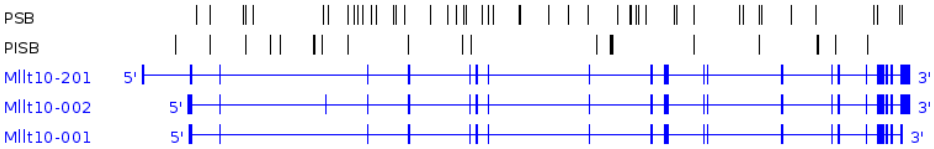

MTMR3 Chr11:4480868-4594863;-

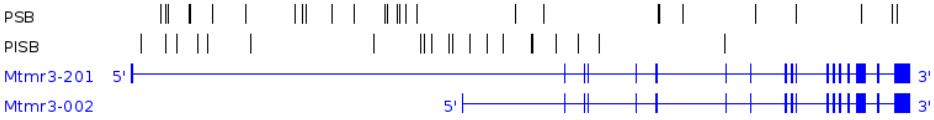

NCOA2 Chr1:13139105-13374083;-

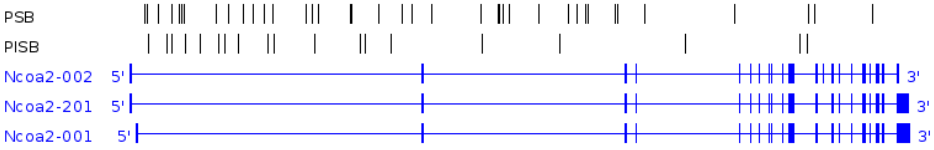

NF1 Chr11:79339693-79581612;+

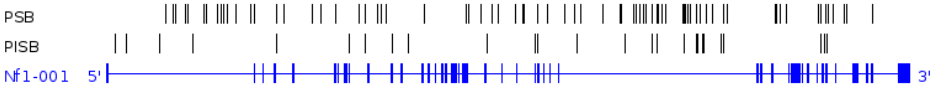

NFIB Chr4:82290173-82705750;-

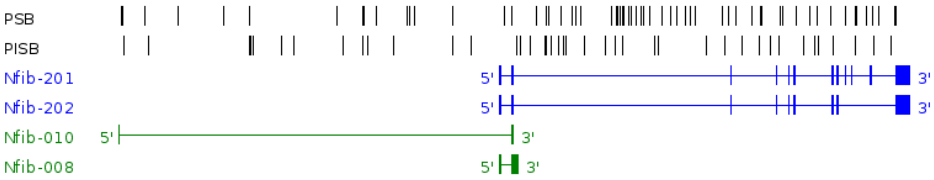

NOTCH1 Chr2:26457903-26516663;-

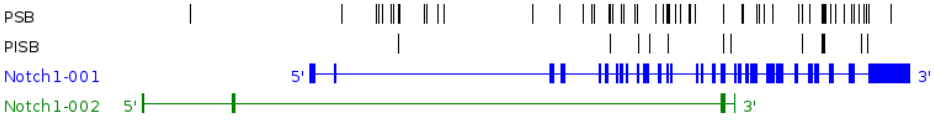

NR3C1 Chr18:39410545-39491301;-

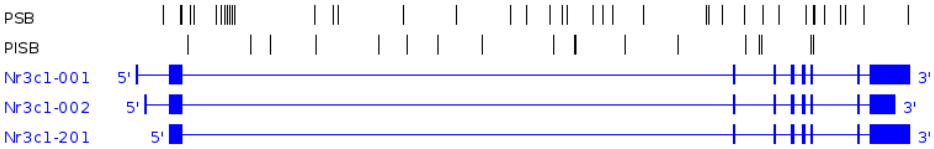

PAFAH1B1 Chr11:74673949-74724670;-

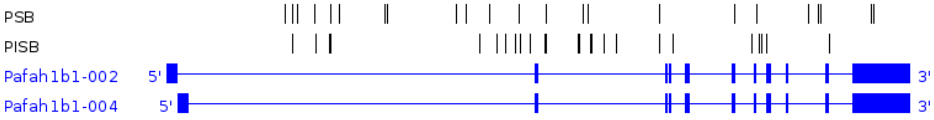

PAIP2 Chr18:35598617-35617186;+

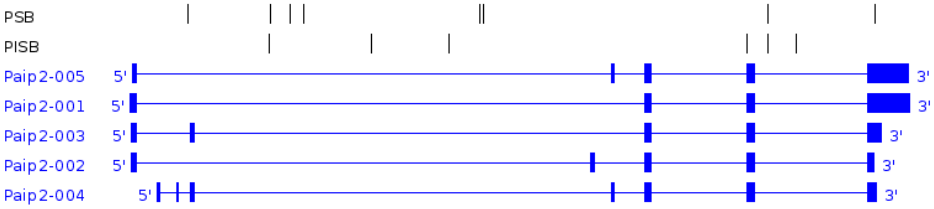

PAK3 ChrX:143518591-143797796;+

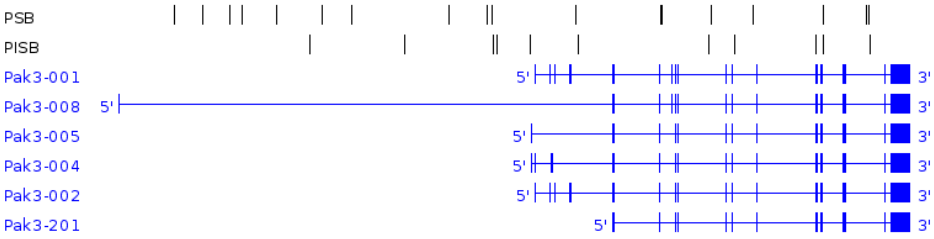

PHIP Chr9:82866159-82975516;-

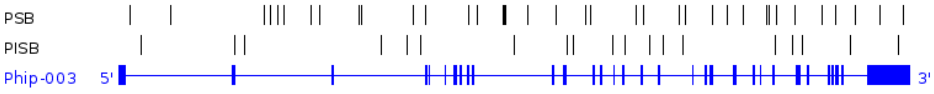

PIAS1 Chr9:62878368-62987924;-

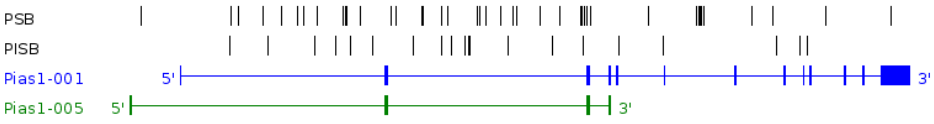

PICALM Chr7:90130213-90213465;+

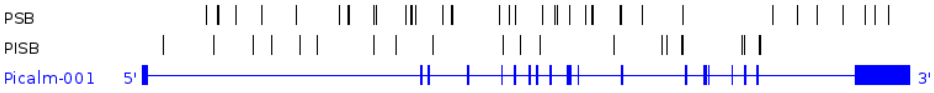

PRL2C2 Chr13:12996132-13005383;-

PRL2C3 Chr13:12790822-12800078;-

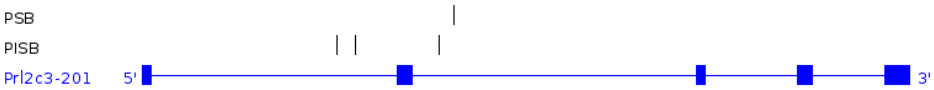

PTBP3 Chr4:59471868-59549364;-

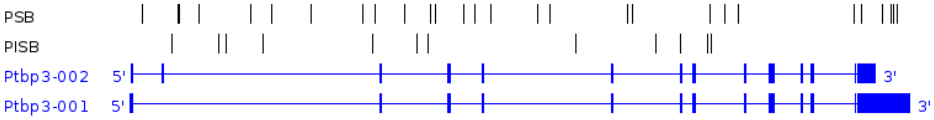

PTPRC Chr1:138062861-138175708;-

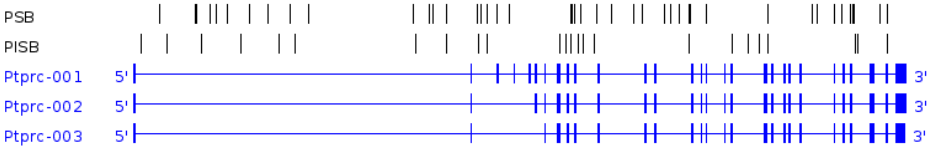

PUM1 Chr4:130663321-130781564;+

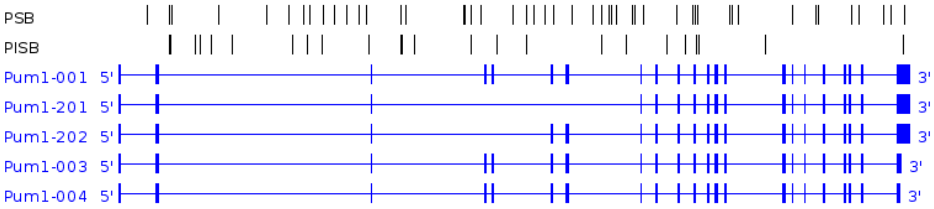

PUM2 Chr12:8674134-8752581;+

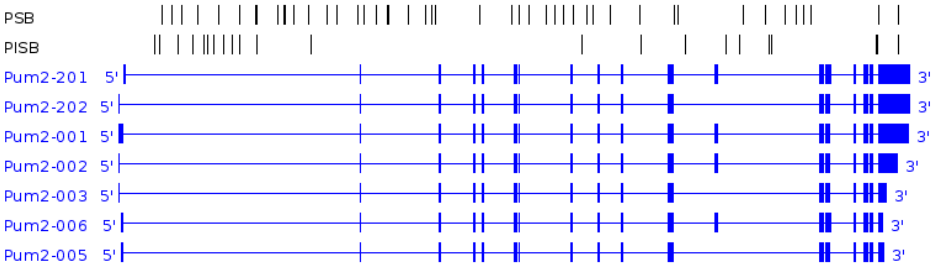

QK Chr17:10206471-10319361;-

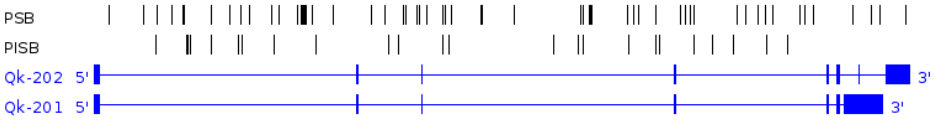

RAB2A Chr4:8535644-8607778;+

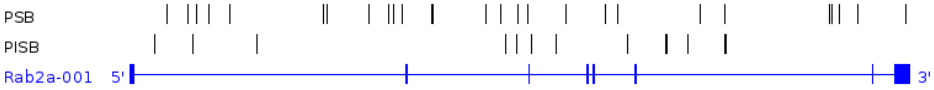

RAB7 Chr6:87999106-88045270;-

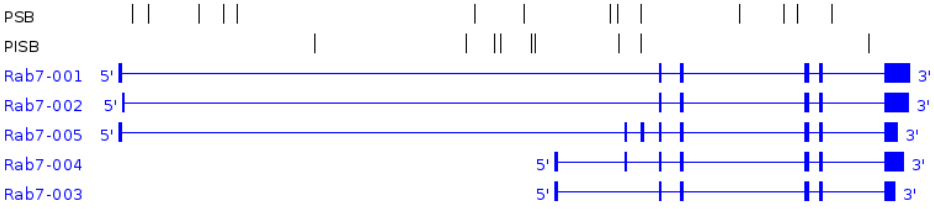

RAD23B Chr4:55350043-55392237;+

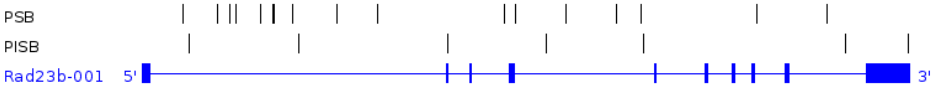

RAP1B Chr10:117814471-117845935;-

RAPGEF2 Chr3:79062516-79286517;-

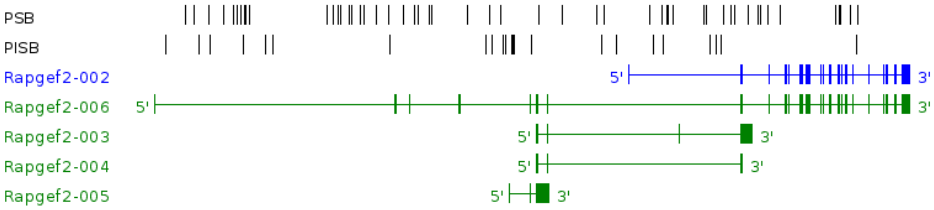

RBM10 ChrX:20617503-20650901;+

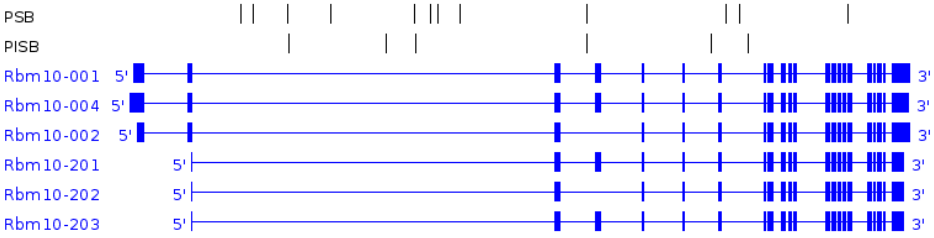

RBM39 Chr2:156147239-156180238;-

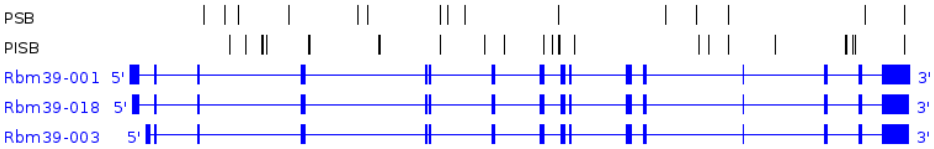

RERE Chr4:150281646-150621966;+

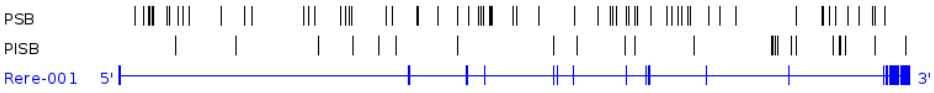

RHOA Chr9:108306129-108337934;+

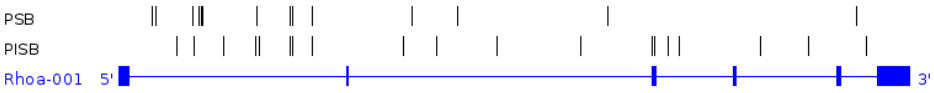

ROCK1 Chr18:10064401-10181792;-

RSF1 Chr7:97579889-97692778;+

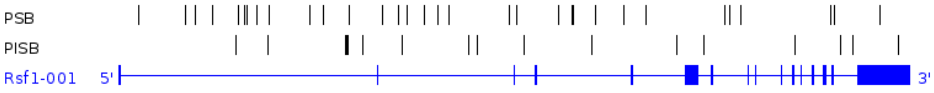

RTN4 Chr11:29692947-29744331;+

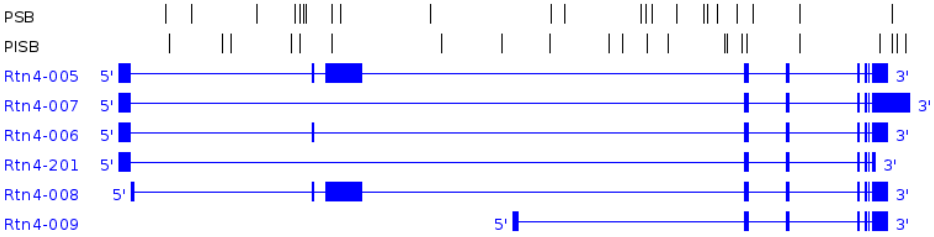

SCAF8 Chr17:3114972-3198855;+

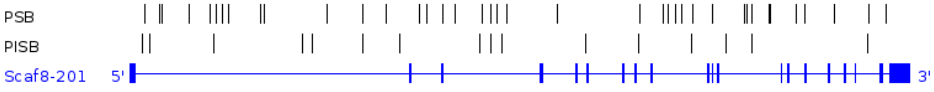

SETD2 Chr9:110532597-110618633;+

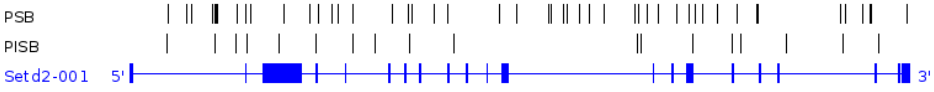

SMG6 Chr11:74925823-75164448;+

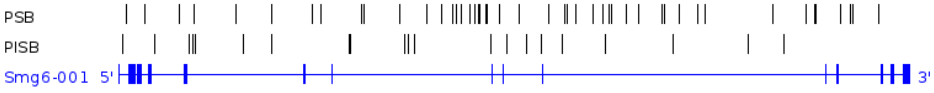

SNRK Chr9:122117266-122169702;+

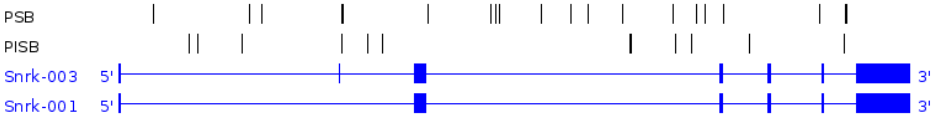

SP3 Chr2:72936427-72980446;-

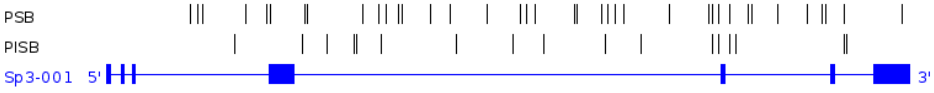

SPPL3 Chr5:115011137-115098790;+

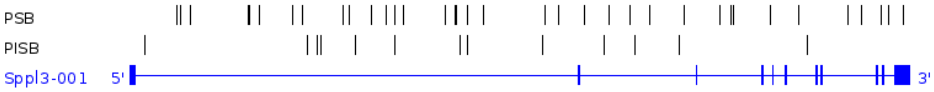

SPRED1 Chr2:117121374-117182279;+

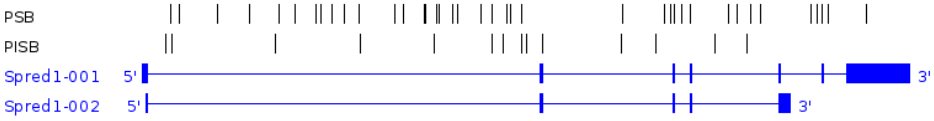

SPTLC2 Chr12:87305058-87388355;-

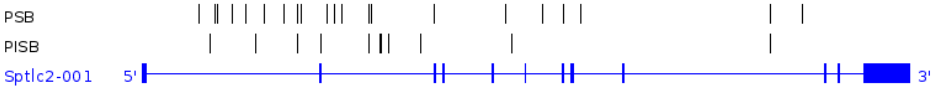

STAG1 Chr9:100597798-100959375;+

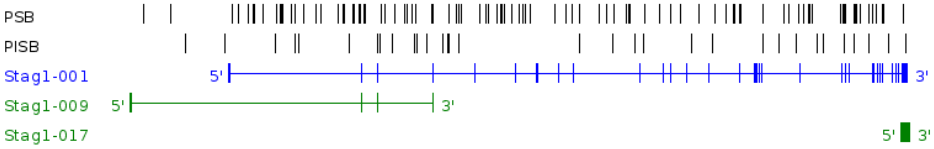

STAG2 ChrX:42149317-42277185;+

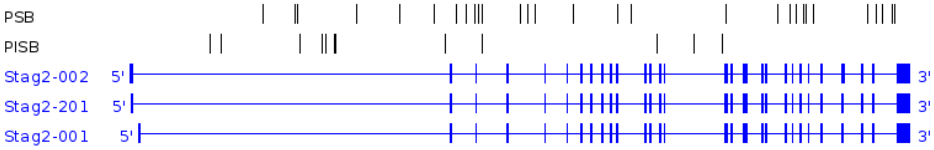

STRN3 Chr12:51608541-51691914;-

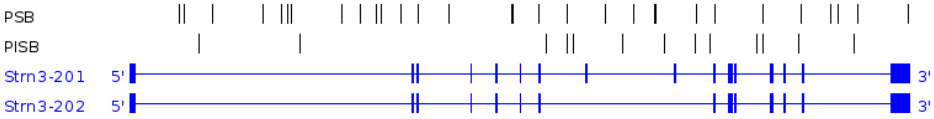

SUSD6 Chr12:80790532-80880832;+

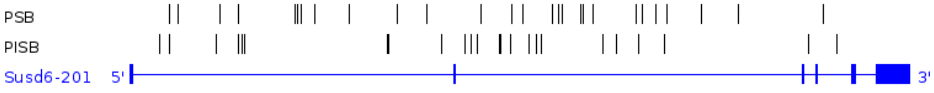

TAOK1 Chr11:77529162-77607815;-

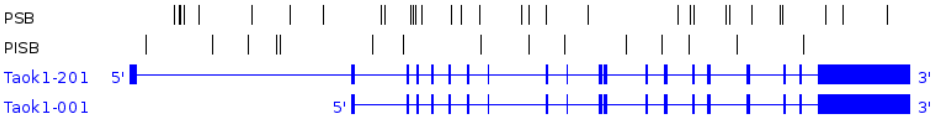

TAX1BP1 Chr6:52713729-52766780;+

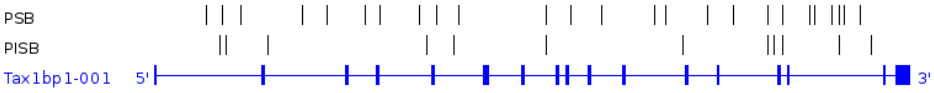

TCF12 Chr9:71842688-72111871;-

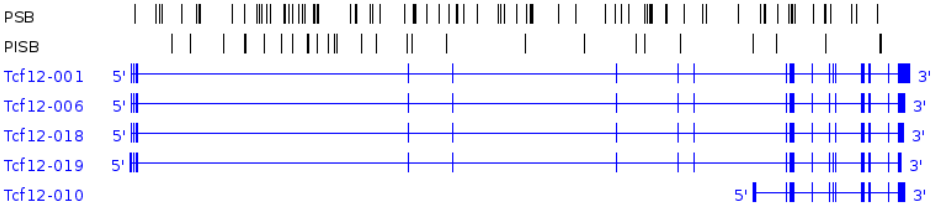

TMEM243 Chr5:9100668-9160986;+

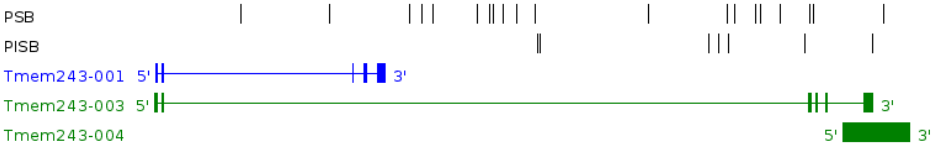

TNRC6B Chr15:80711319-80941086;+

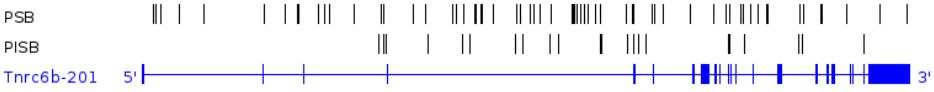

TOP1 Chr2:160645888-160722764;+

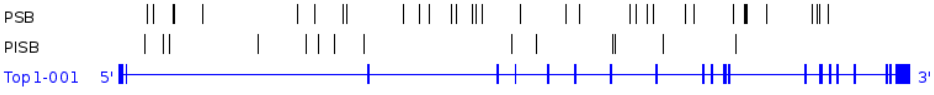

UBAP2L Chr3:90000140-90052628;-

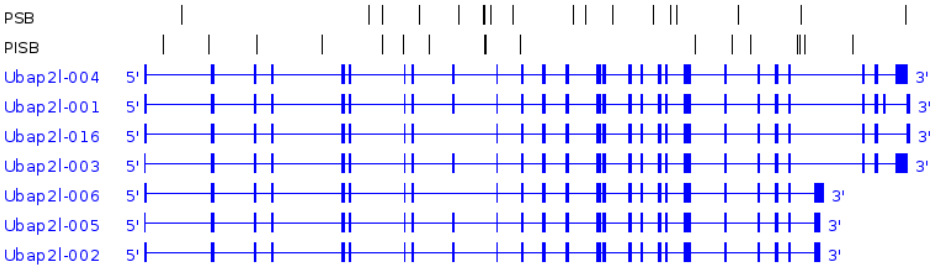

UBE2D2A Chr18:35771559-35807172;+

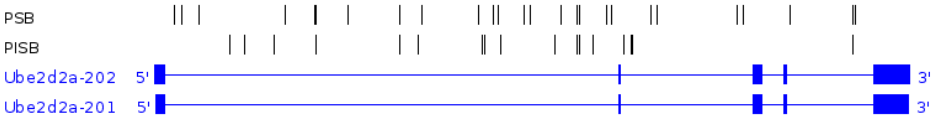

UBE2D3 Chr3:135438149-135468198;+

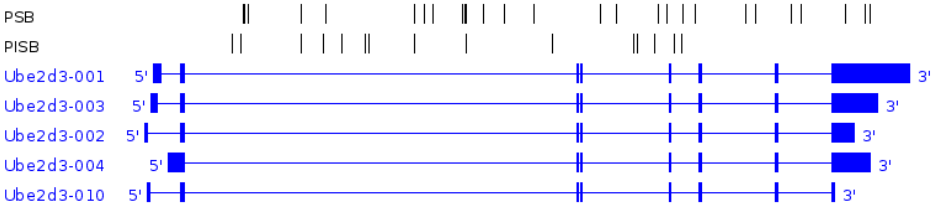

UBE2K Chr5:65537233-65598988;+

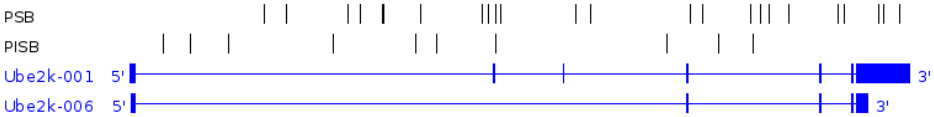

UBE2N Chr10:95515162-95545658;+

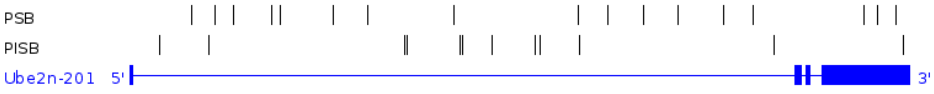

USP34 Chr11:23306895-23490560;+

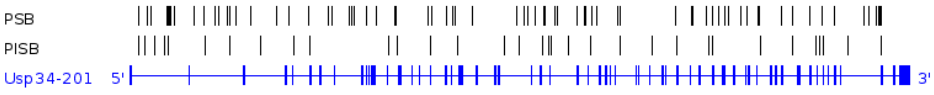

USP9X ChrX:13071498-13173328;+

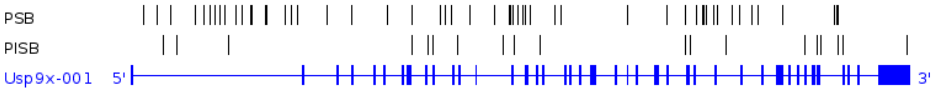

USP9Y ChrY:1298961-1459782;-

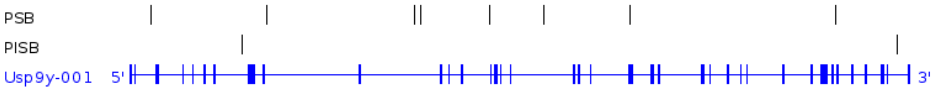

UTY ChrY:1096861-1245759;-

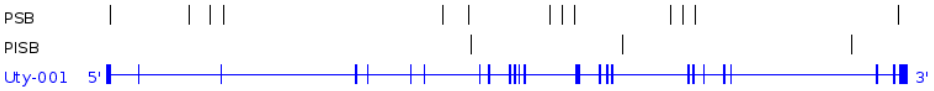

VMN2R-PS139 ChrY:4005164-4016574;+

WAC Chr18:7868832-7973547;+

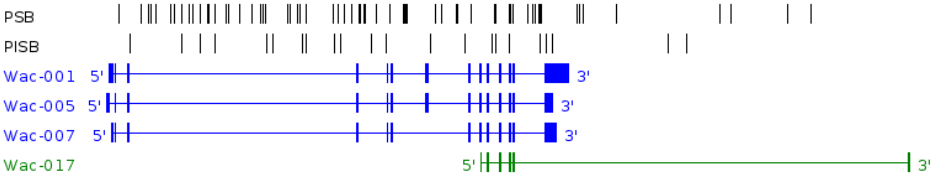

YTHDF3 Chr3:16183212-16217037;+

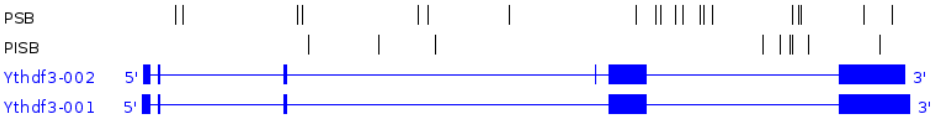

YWHAE Chr11:75732869-75765845;+

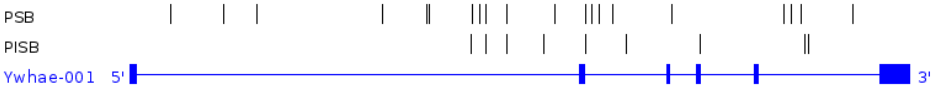

YWHAZ Chr15:36770770-36794547;-

ZBTB11 Chr16:55973883-56008913;+

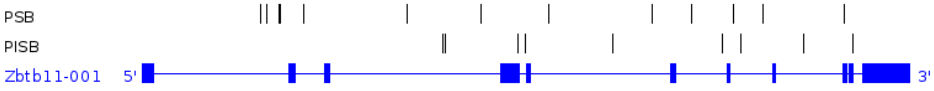

ZFAND3 Chr17:30005087-30210019;+

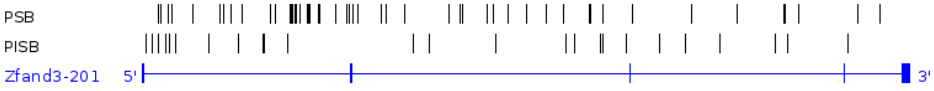

ZFP148 Chr16:33380775-33503903;+

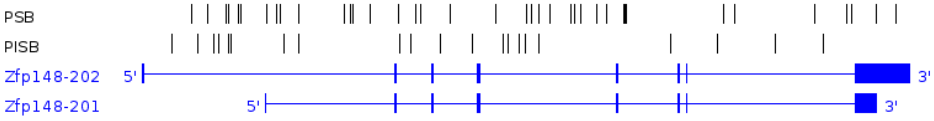

ZFP207 Chr11:80383279-80405733;+

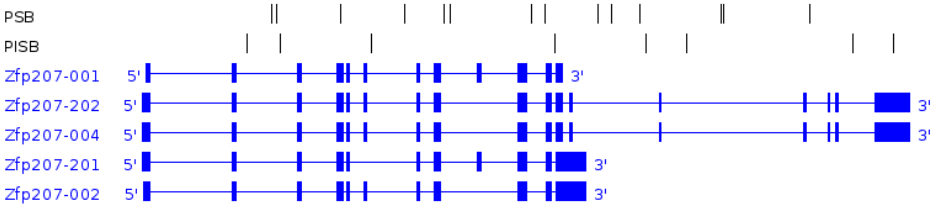

ZFP609 Chr9:65692391-65827564;-

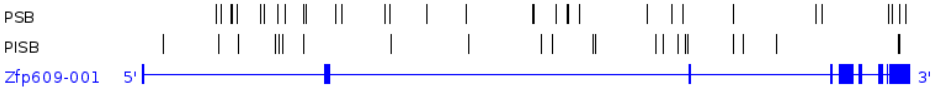

ZMYND11 Chr13:9684836-9765321;-

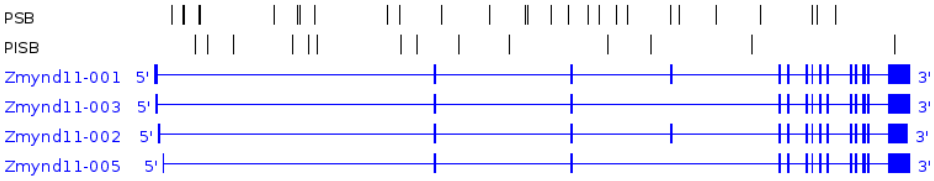

Supplementary Figure 7. Transposon integration pattern across the PSB∩PISB CIS genes in PSB and PISB skin tumors. Only the transposon insertions falling in the genes nearest to the center of each CIS peak are represented. For these genes, only the consensus CDS (CCDS) transcripts are shown (blue) unless these cover less than 98% of the annotated gene length, in which case non-CCDS transcripts are also depicted (green). Genes without insertions correspond to the gene closest to the center of an intergenic CIS.

a

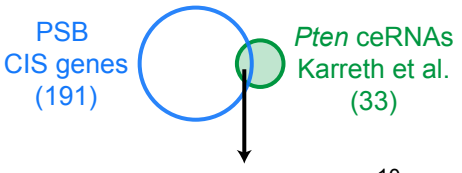

8 (4%), $P = 6.58 \times 10^{-10}$

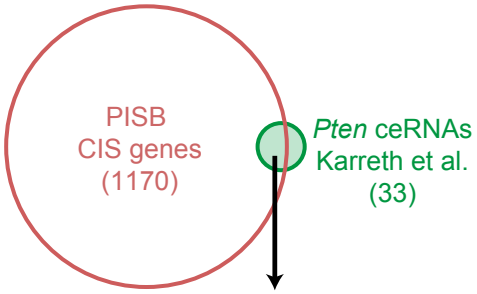

21 (2%), $P < 2.2 \times 10^{-16}$

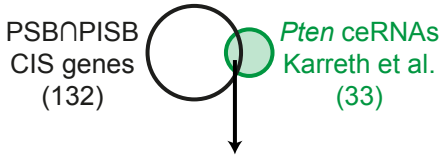

8 (6%), $P = 3.63 \times 10^{-11}$

b

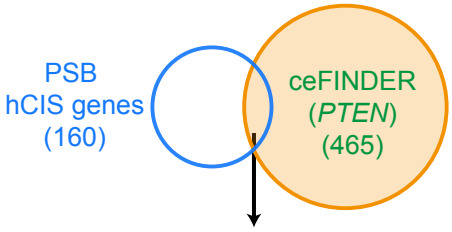

23 (14%), $P = 4.51 \times 10^{-12}$

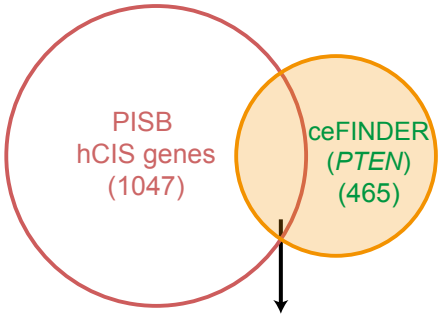

120 (11%), $P < 2.2 \times 10^{-16}$

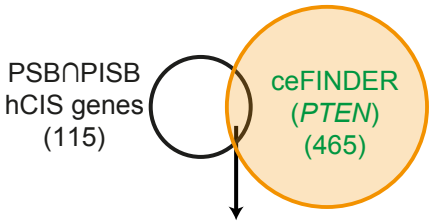

18 (16%), $P = 2.44 \times 10^{-10}$

Supplementary Figure 8

Supplementary Figure 8. Identification of known and putative *PTEN* competitive endogenous RNAs (ceRNAs). PSB, PISB and PSB∩PISB CIS/hCIS genes are significantly enriched in *PTEN* ceRNAs previously reported by Karreth et al. **(a)** and predicted by the ceFINDER algorithm **(b)**. The number of genes included in each group/dataset is indicated. Mouse genes or human genes whose mouse orthologues map to chromosomes 14 and 19 were not included in the analysis. Percentages in parenthesis represent the proportion of PSB, PISB or PSB∩PISB CIS/hCIS overlapping with each one of the two datasets. *P* values were calculated using a two-by-two contingency table and Fisher's exact test.

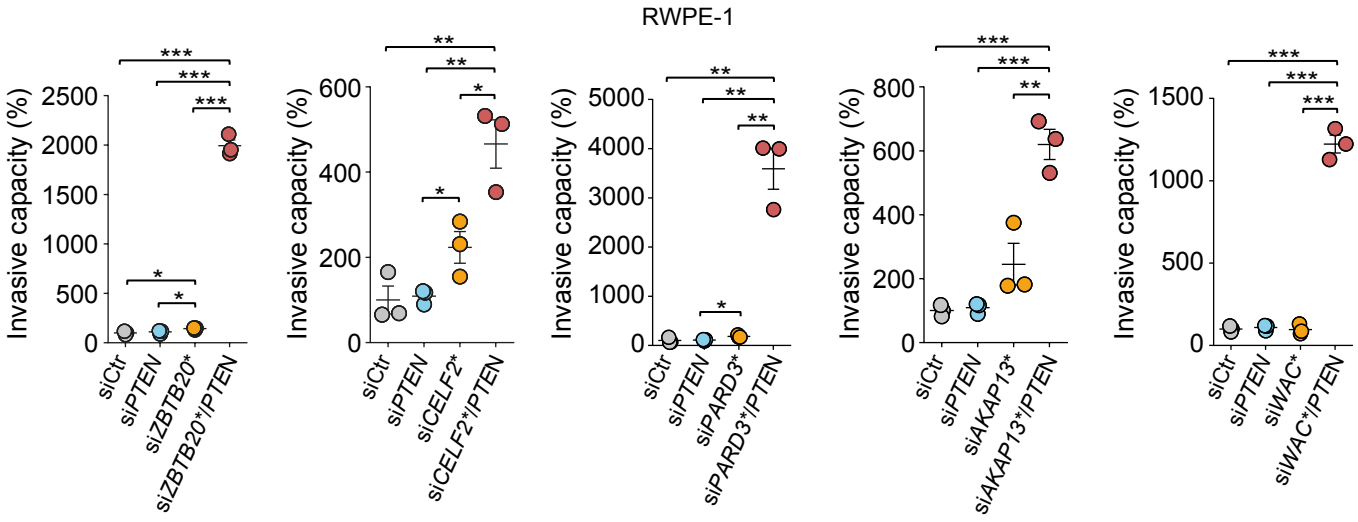

Supplementary Figure 9

Supplementary Figure 9. Effect of *ZBTB20*, *CELF2*, *PARD3*, *AKAP13* and *WAC* silencing, either alone or in combination with *PTEN* interfering, on the invasiveness of the RWPE-1 immortalized human prostate cell line. Alternative siRNAs to those of Figure 4 were used. Cell invasion rate is expressed as a percentage relative to the mean of control invasion rate values, which was set as 100%. Each circle represents an individual technical replicate. Horizontal lines represent the means and error bars correspond to s.e.m in each condition. $*P < 0.05$, $**P < 0.01$, $***P < 0.001$, two-tailed Student's t test.

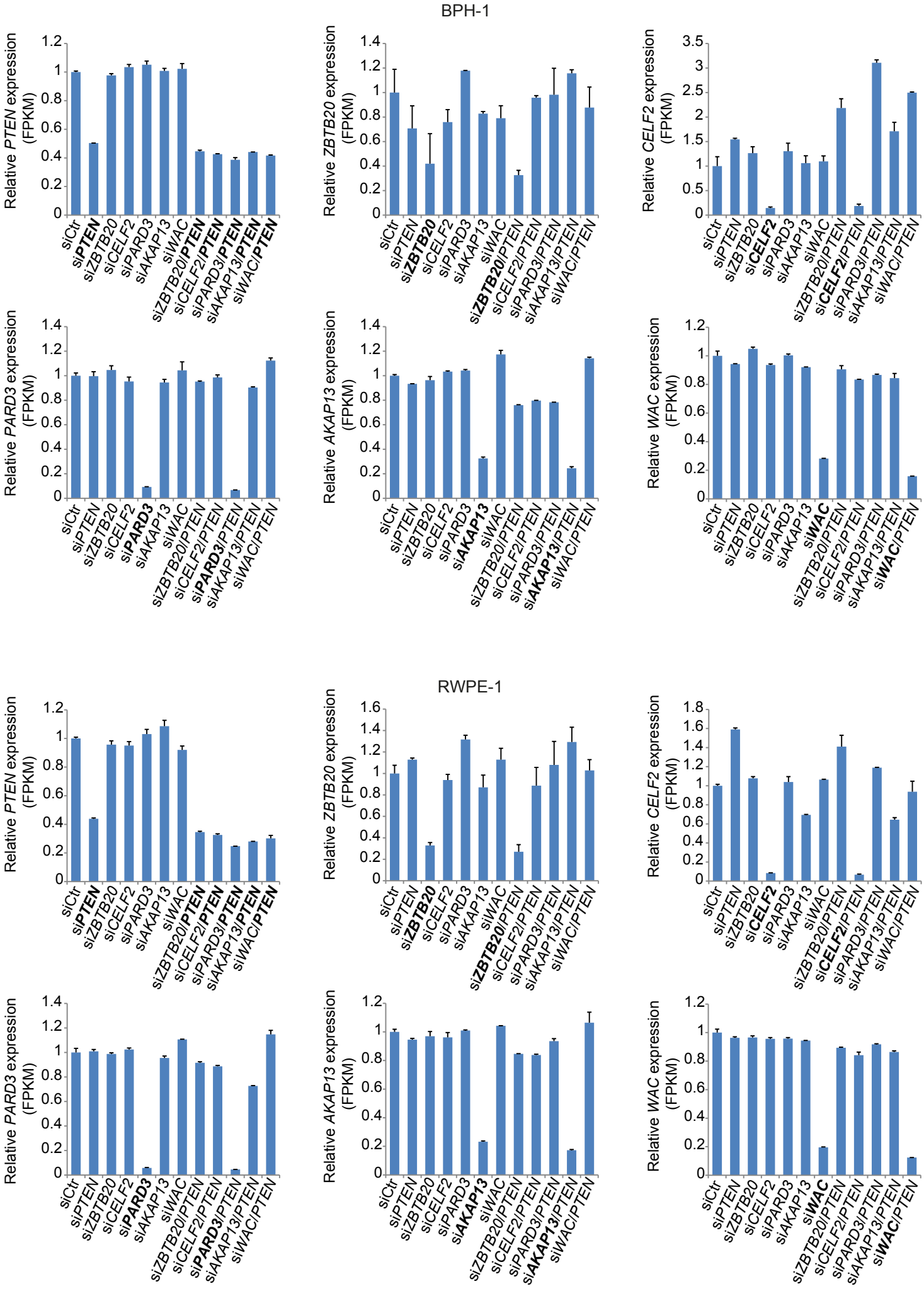

Supplementary Figure 10

Supplementary Figure 10. Relative mRNA expression of *PTEN*, *ZBTB20*, *CELF2*, *PARD3*, *AKAP13* and *WAC* in all co-silencing and single-silencing conditions in BPH-1 and RWPE-1 cell lines. FPKM values were used.

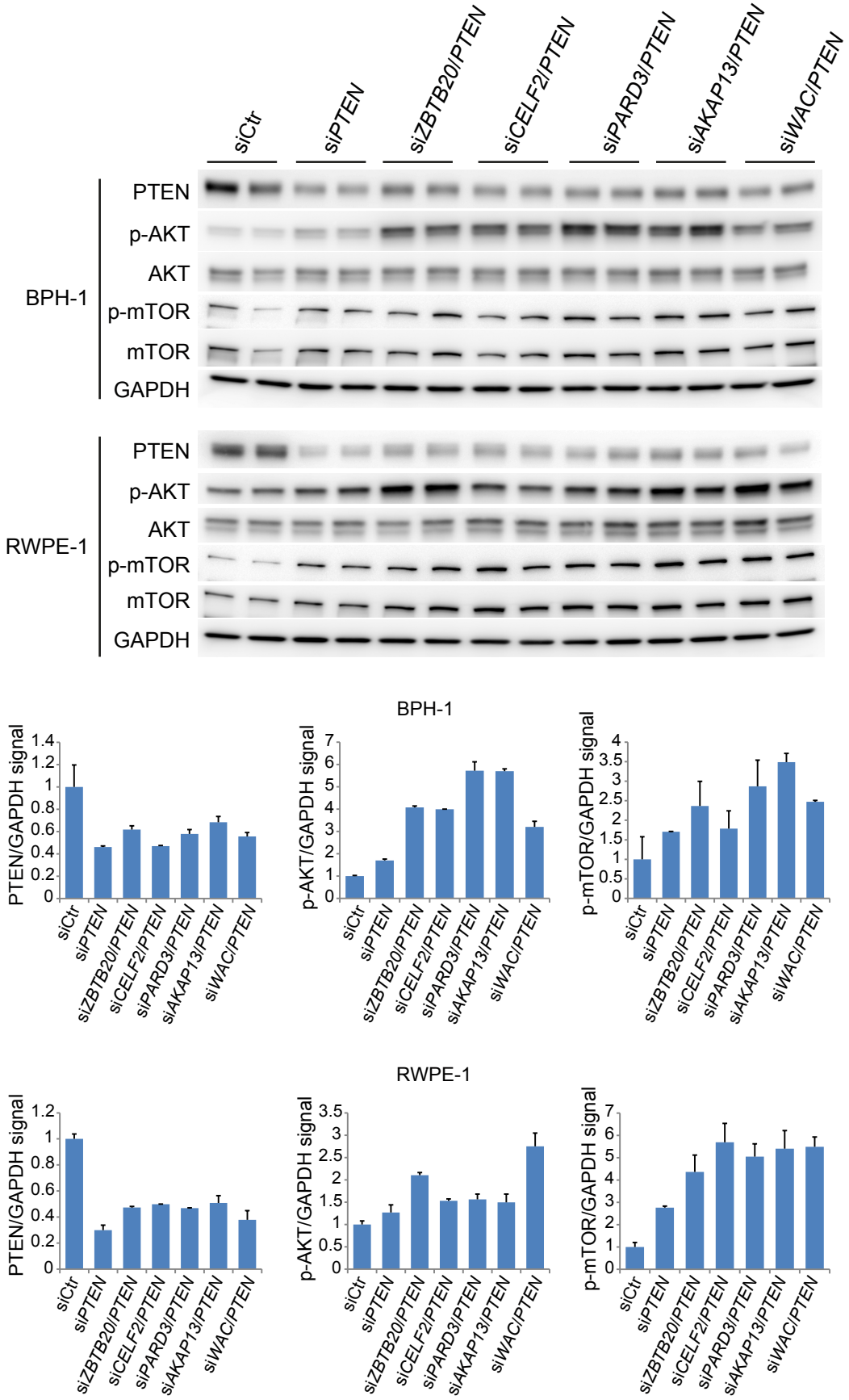

Supplementary Figure 11

Supplementary Figure 11. Western blot analysis of the PI3K/AKT/mTOR signaling pathway in BPH-1 and RWPE-1 cells upon co-silencing of *ZBTB20*, *CELF2*, *PARD3*, *AKAP13* and *WAC* with *PTEN*. Upper panel: Western blot analysis of PTEN, p-AKT, AKT, p-mTOR, mTOR and GAPDH is shown for each of the conditions examined. Lower panel: densitometry analysis of the immunoblots. GAPDH was used for protein level normalization.

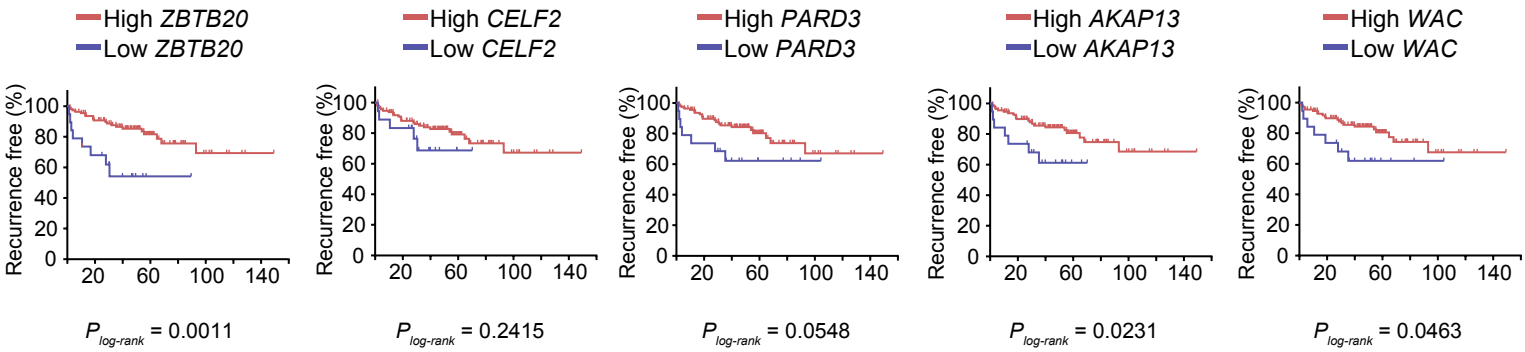

Supplementary Figure 12

Supplementary Figure 12. Recurrence-free survival Kaplan-Meier analysis of the 15% of patients with lowest mRNA expression levels of each of the five genes selected for validation versus the remaining 85%. Only patients with primary tumors were taken into account. Analyses were performed using the Taylor dataset and the open web interface 'Project Betastasis' (http://www.betastasis.com). P values were obtained by log-rank test.

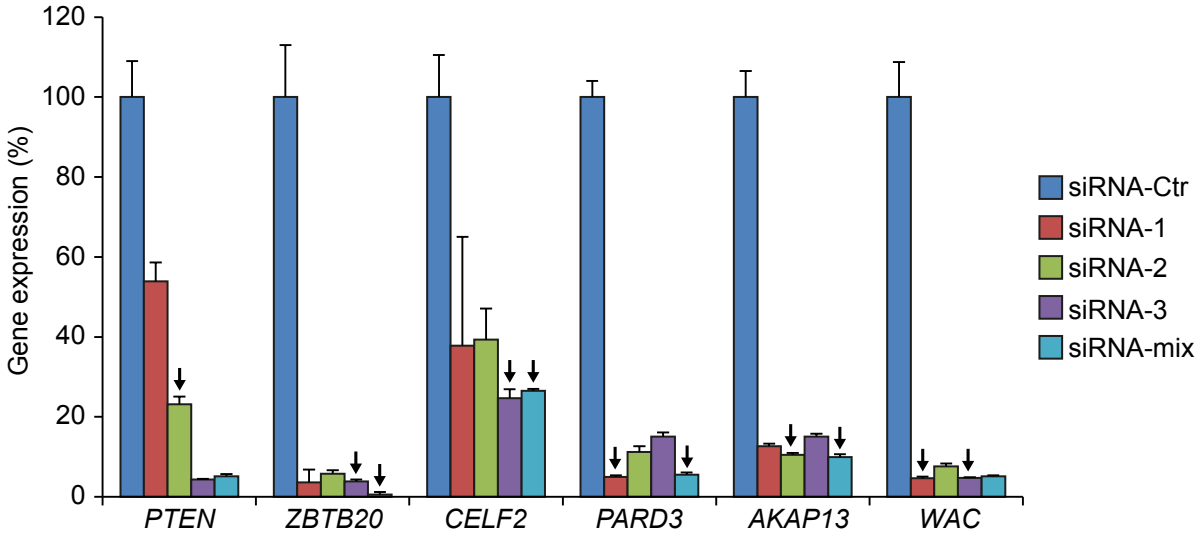

Supplementary Figure 13

Supplementary Figure 13. Knockdown efficiency of *PTEN*, *ZBTB20*, *CELF2*, *PARD3*, *AKAP13* and *WAC* silencing in BPH-1 cells. Three different siRNAs or a combination of the three were tested per each gene. Gene silencing efficiency was evaluated by quantitative PCR (qPCR) and represented as a percentage relative to control siRNA-transfected cells, which was set as 100%. Arrows indicate those conditions selected for each gene for subsequent studies. Results are expressed as mean ± s.d.